A general size- and trait-based model of plankton communities

Serra-Pompei, Camila; Soudijn, Floor ; Visser, André W.; Kiørboe, Thomas; Andersen, Ken Haste

Published in:
Progress in Oceanography

Link to article, DOI:
10.1016/j.pocean.2020.102473

Publication date:
2020

Document Version
Peer reviewed version

A general size- and trait-based model of plankton communities

Camila Serra-Pompei[1], Floor Soudijn[2], André W. Visser[1], Thomas Kiørboe[1], and Ken H. Andersen[1]

[1]Centre for Ocean Life, Technical University of Denmark, DTU Aqua, Kemitorvet B201, Kongens Lyngby 2800, Denmark

[2]Ecological Dynamics Group, Wageningen Marine Research, Haringkade 1, 1976 CP IJmuiden, The Netherlands

Keywords: copepod, model, NPZ, trait, plankton, zooplankton.

Corresponding author contact information: Camila Serra-Pompei. Email: mcsp@aqua.dtu.dk. Address: Kemitorvet, Building 202, 2800 Kgs. Lyngby, Denmark.

Abstract

Multicellular zooplankton, such as copepods, are the main link between primary producers and fish. Most models of plankton communities, such as NPZ-type models, ignore the life-cycle (ontogeny) of multicellular zooplankton. Ontogeny has profound implications on population dynamics and community structure. Our aim is to provide a generic food-web framework of planktonic communities that accounts for zooplankton ontogeny. We propose a model framework along the Nutrient-Unicellular-Multicellular axis – a "NUM" framework – as an alternative to the NPZ modelling paradigm. NUM is a mechanistic size- and trait-based model based on traits and trade-offs at the individual level. Here the multicellular component describes the population dynamics of key copepod groups, characterized by their adult size and feeding mode. The unicellular compartment accounts for auto- mixo- and heterotrophic protists. We also consider nitrogen dynamics and carbon export from copepod fecal pellets. All parameters have been fitted to cross-species data. By approximate analytical solutions and dynamic simulations, in both constant and seasonal environments, we investigate the patterns of body sizes and traits that emerge within the community. We show that copepods of several adult sizes and feeding modes commonly coexist, and that competition and predation by large copepods on small/juvenile copepods is an important factor in shaping the community. We also show competition between heterotrophic protists and small copepods through intraguild predation. Finally, we discuss how copepods can attenuate the fecal pellet export. This conceptually simple, yet realistic framework opens the possibility to improve end-to-end size-structured models of marine systems and investigate biogeochemical processes.

1 Introduction

Planktonic organisms weave an intricate web of trophic pathways channelling energy and matter within a richly diverse community. These complex food webs are often simulated by a simple NPZ model: a compartmentalized trophic chain reduced to interactions between nutrients, autotrophs and heterotrophs (Franks, 2002; Gentleman, 2002). In the simplest case, NPZ models have only three compartments: nitrogen, phytoplankton, and zooplankton (e.g. Evans and Parslow, 1985). Introduction of additional nutrients and autotroph and heterotroph compartments adds realism at the cost of a larger parameter set (e.g. Fasham, Ducklow, and McKelvie, 1990). The number of parameters can be reduced by simulating a large number of generalized plankton populations with parameters based on statistical trade-offs between life-history parameters (Follows and Dutkiewicz, 2011). Together, such models have given considerable insights into the bio-geochemistry of the oceans (Weitz et al., 2015). However, extending models to higher trophic levels, particularly towards fish and fisheries, remains elusive (Fulton, 2010), in part because of an incomplete representation of zooplankton (Mitra et al., 2014).

The zooplankton compartment in NPZ models generally represents the biomass of two types of organisms: protists (heterotrophic flagellates and ciliates) and meso-zooplankton (mainly copepods). An important distinction between these two groups that is ignored by NPZ models is that protists reproduce by cell division, whereas meso-zooplankton grow through different life stages, often spanning several orders of magnitude in mass (Neuheimer et al., 2015). This ontogenetic development changes the trophic position of an individual — both in what it eats and what seeks to eat it (Werner and Gilliam, 1984). Such ontogenetic niche shifts introduce several effects. Examples are: (i) bottlenecks in life-stages if availability of prey is low (de Roos and Persson, 2013a), (ii) cannibalism (Bonnet, Titelman, and Harris, 2004), (iii) or intraguild predation (Polis, Myers, and Holt, 1989; Gismervik and Andersen, 1997). Further, (iv) cyclic cohort dynamics (McCauley and Murdoch, 1987; Persson et al., 1998) and time delays (May, 1973) due to the development of individuals, for instance between the emergence of juveniles and peak consumption by adults. In a seasonal pelagic environment this time delay is one of the factors leading to spring blooms (Kiørboe, 1993; Longhurst et al., 1995; Behrenfeld and Boss, 2014). None of these effects are resolved by a model where zooplankton populations, or groups of populations, are represented as single state variables.

Models of the unicellular community may represent the diversity of organisms – both P and Z

compartments – by a size distribution (Banas, 2011; Ward and Follows, 2016; Ho et al., 2019). A particular advantage of this approach is its ability to represent various degrees of mixotrophy; since many unicellular organisms are neither purely autotrophic ("P") or heterotrophic ("Z") (Flynn and Hansen, 2013). Some further representation of diversity can be introduced in the form of functional groups (Leles et al., 2018) or functional traits, such as investment in resource uptake or vacuoles (Chakraborty, Nielsen, and Andersen, 2017; Hansen and Visser, 2019). As copepods are largely size-selective feeders (Kiørboe, 2016), a unicellular size-distribution model presents a suitably structured representation of the food for copepods.

In this work we propose a model framework along the Nutrient-Unicellular-Multicellular axis – a "NUM" framework – as an alternative to the NPZ modelling paradigm. A particular focus is to include the life history of multicellular zooplankton organisms. Size is a key trait as it governs physiological rates and predator-prey interactions (e.g. Kiørboe and Hirst, 2014; Andersen et al., 2016; Kiørboe, 2016), both among the unicellular auto-, mixo- and heterotrophs in the "U" component and the multicellular plankton "M". The unicellular community is represented solely by cell size, and their trophic strategy is an emergent property. For multicellular plankton, body size is used to resolve the population structure from nauplii to adult copepods, and further diversity is introduced by functional traits. We use a generic food-web framework (Hartvig, Andersen, and Beyer, 2011) to represent ontogenetic growth with size at maturation as a key trait. This framework is based on physiologically structured models (de Roos and Persson, 2013b) and describes the life-cycle of organisms based only on processes at the level of individual organisms. Here, we include feeding mode as an additional important trait of copepods. Copepods can be active or passive feeders (Kiørboe, 2011). Active feeders have a high-risk high-gain strategy where they constantly search for food, making them vulnerable to detection by predators. Passive "sit-and-wait" feeders have a lower intake of food and metabolic expenditure but are also less exposed to predation. Overall, the basis for the NUM framework is a combination of size- and trait-based modelling (Hartvig, Andersen, and Beyer, 2011; Kiørboe, Visser, and Andersen, 2018).

We first present analytical solutions of the community and multicellular components in terms of ontogenetic growth rates, development time, population and community structure, and population growth rates. We then investigate how the size- and trait-structure of the emerging community responds to changes in the environmental drivers, mainly nutrients. Finally, due to the large contribution of copepods for carbon export (Ducklow, Steinberg, and Buesseler, 2001; Stamieszkin et al.,

2015; Steinberg and Landry, 2017), we use the NUM model to estimate the carbon export originating from copepod fecal pellets.

2 Methods

The model has four compartments (fig. 1 c and d): (i) a size- and trait-structured copepod community, (ii) a size-structured community of unicellular protists, (iii) a single dissolved nitrogen pool, and (iv) a size-structured pool of fecal pellets. Protists perform photosynthesis, take up nitrogen, and eat other protists. Copepods eat protists, other copepods, and fecal pellets. The copepod community (fig. 1c) consists of populations of copepods characterized by their traits: adult size and feeding mode. All processes of protists and copepods are described at the individual level (fig. 1a), i.e., food encounter, consumption, assimilation, respiration, growth, and reproduction. In the following sections we first describe the individual-level energy budget and how it depends on body mass (section 2.1). Next, we describe the main traits for the copepods and show how the traits influence the parameters (table 1 and Appendix B) in the energy budget (section 2.2). The individual-level description is scaled up to the population-level by solving continuous or discrete formulations of the McKendric-von Foerster equation (fig. 1b, section 2.3 and Appendix F). Finally, we show the size-based protist model (section 2.5 and Appendix B.2) and the full bio-geochemical model (fig. 1d and section 2.7).

2.1 Copepod energy budget

The energy budget of an individual copepod (fig. 1a) describes the capture and assimilation of food and how it is used for growth and reproduction (Hartvig, Andersen, and Beyer, 2011). Physiological rates scale with the body-mass of the copepod. Most of the rates used in the model are mass-specific and not per individual. The body-mass of a copepod changes over its life, and we refer to it as a state. This is different from the traits that we use to describe a population. A copepod population is described by the feeding mode and the adult body mass (and not copepod body-mass at any stage). In this section we will first describe the mass dependency of the energy budget, and in the next section we will explain the traits used to describe a population and how the parameters depend on the feeding mode.

Food availability $E(m)$ (µgC L^{-1}) depends on copepod body mass (m) and on the abundance and size distribution of the community (further explained in section 2.4). The encounter rate of food

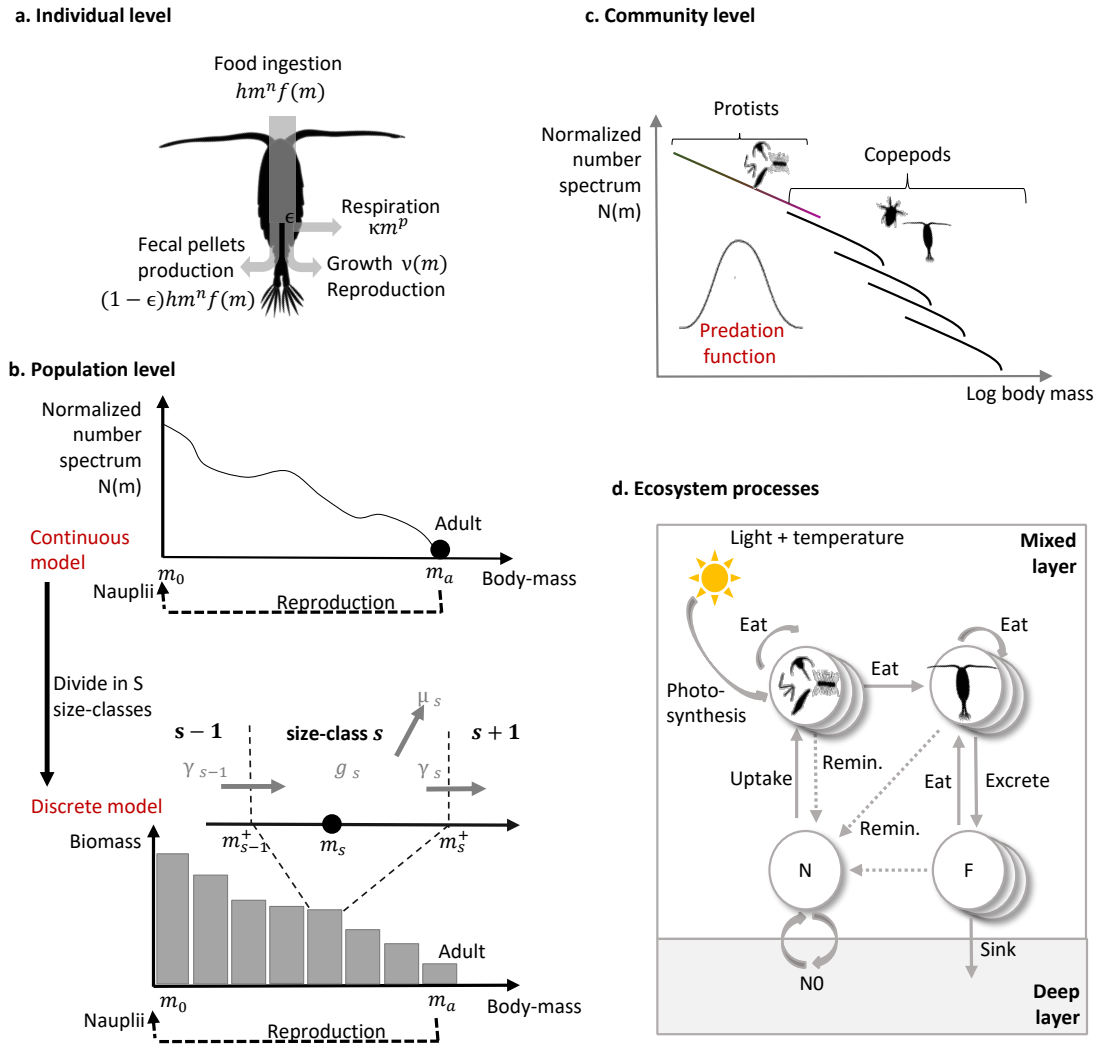

Fig. 1. Diagram of each section of the model. **a**, processes at the individual level (section 2.1). Food that is assimilated covers metabolic costs and is used for growth and reproduction; and non-assimilated food is excreted in the form of fecal pellets. **b**, population model used in section 2.3, in the continuous and the stage-structured representations. Notations in grey show the rates that affect each size class s: somatic growth (γ), biomass accumulation within the size class (g), and mortality (μ). **c**, community level (section 2.4). The community is composed of a size spectrum of protists (sec. 2.5), and a number of copepod populations. **d**, Ecosystem interactions (sections 2.4 and 2.7). Here "N" and "F" represent the nutrient pool and fecal pellet size spectrum.

(d^{-1}) is found by multiplying the available food with the clearance rate vm^q (L d^{-1} µgC^{-1}). Ingestion rate is limited by the maximum ingestion rate hm^n (d^{-1}). A measure of the level of satiation of an organism is the feeding level $f(m)$ (dimensionless). The feeding level ranges from 0 to 1, with 1 being

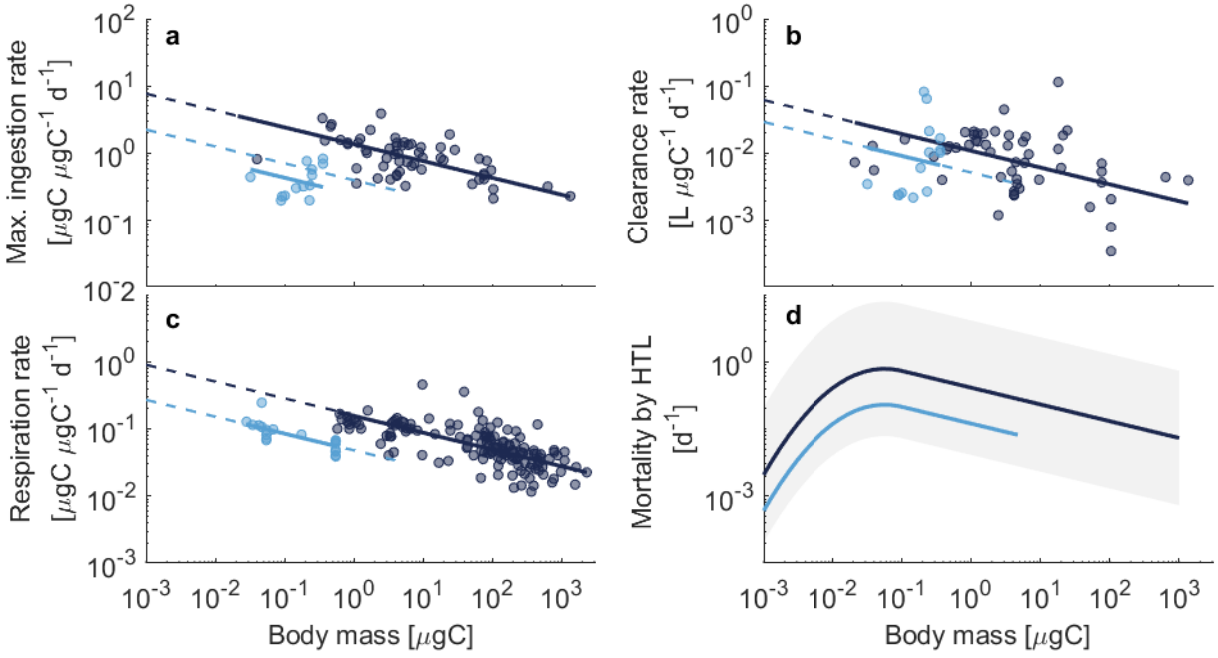

Fig. 2. Parameter values for active (dark blue) and passive (light blue) copepods. (**a,b,c**) Dots are data from Kiørboe and Hirst (2014) (see Appendix B for conversion factors), and solid lines are linear least square regression fits (forced slope of -1/4),dashed lines are parameter values used in the model after corrections (such as discussed in the text and Appendix B). (**a**) Maximum ingestion rate (hm^n), (**b**) clearance rate (vm^q) and (**c**) respiration rate (κm^p). (**d**) Mortality by higher trophic levels imposed in the model as a closure term. The mortality is density-dependent and can vary, as illustrated with the shaded area.

full satiation, and is described as:

$$f(m) = \frac{\overbrace{vm^q E(m)}^{\text{Encounter rate}}}{\underbrace{vm^q}_{\text{Clearance rate}} \quad E(m) + \underbrace{hm^n}_{\text{Maximum ingestion rate}}} \quad . \tag{1}$$

where q and n are exponents reflecting allometric scaling of clearance rate and ingestion rate respectively. Note that when multiplied by the maximum ingestion rate, a type II functional response is obtained.

The specific biomass production rate $\nu(m)$ (d^{-1}) is defined as the energy available after food assimilation and respiration (κm^p in d^{-1}):

$$\nu(m) = \epsilon \underbrace{hm^n f(m)}_{\text{Ingestion rate}} - \underbrace{\kappa m^p}_{\text{Respiration rate}} \quad , \tag{2}$$

where ϵ is the assimilation efficiency, and κ and p are the coefficient and exponent of the respiration rate.

We define the "critical feeding level" (f_c) as the feeding level where organisms start to starve, i.e., where assimilation of food equals respiration:

$$f_c(m) = \frac{\kappa}{\epsilon h} m^{p-n}. \tag{3}$$

Note that when the exponents of maximum ingestion and respiration are identical, $n = p$, the critical feeding level is independent of body size. Combining equations 2 and 3, the specific biomass production rate $\nu(m)$ (d^{-1}) can be re-written as:

$$\nu(m) = \epsilon h m^n (f(m) - f_c(m)). \tag{4}$$

If the net energy gain is positive, i.e. if food assimilation surpasses respiration, the energy is invested into somatic growth or reproduction. Thus, the net energy gain $g(m)$ (d^{-1}) becomes:

$$g(m) = \max[0, \nu(m)]. \tag{5}$$

If the biomass production rate ν is negative, i.e., if respiration exceeds food assimilation, then we need to account for the respiration losses that are not covered by ν. We do that by imposing a "starvation loss" term on the biomass (as in de Roos et al., 2008):

$$\mu_{st}(m) = \min[0, \nu(m)], \tag{6}$$

which is only relevant when $\nu(m) < 0$.

Adults use the net energy gain to reproduce, and the birth rate of nauplii (d^{-1}) equals:

$$b = \epsilon_r g(m_a), \tag{7}$$

where $g(m_a)$ is the net energy gain of adults. ϵ_r is the reproduction efficiency, and takes into account the eggs survival and the male:females ratio (see Appendix B).

The central physiological parameters, clearance rate, respiration rate, and maximum ingestion rate are given in figure 2. For all parameters we fixed the size-scaling exponents to $-1/4$ as explained in Appendix B. Note that the scaling is negative since most rates are mass-specific, i.e per unit of carbon mass and not per individual.

2.2 Copepod traits

We proceed on the premise that the functional diversity of copepods can be well represented by two key traits: their adult mass (m_{a}) and their feeding mode (active/passive). Both of these traits affect copepod fitness through mechanistic links to other life-history parameters.

The adult body mass determines the size range of the population, since offspring mass (m_0) is proportional to the adult mass (Neuheimer et al., 2015): $m_a = z_{\mathrm{a:o}} m_0$, where $z_{\mathrm{a:o}}$ is the adult-to-nauplii mass ratio. The body-mass range of adult copepods chosen here is of 0.2 µgC to 1000 µgC for active feeders and 0.2 µgC to 5 µgC for passive feeders. The extremes of the size range correspond to adult copepods between 0.2 mm and 7 mm (assuming the mass-length relationships of Chisholm and Roff, 1990, fig. B.3).

The differences between feeding modes appear in the coefficients of the physiological parameters (fig. 2) and the predation mortality. The passive feeding strategy implies that copepods have to maintain neutral buoyancy in the water column, which allows them to be undetected by predators. We argue that large copepods are too heavy to maintain neutral buoyancy and have to constantly swim to do so. This could explain why in nature most passive feeders are small in size (e.g. *Oithona sp.*). Higher predation and respiration rates for large passive feeders can be introduced in the model following assumptions regarding sinking and swimming speeds (see Appendix E). However, in the runs presented here we will limit the size range of passive feeders to reduce the number of state variables.

Passive feeding copepods have been suggested to experience predation mortality that is about 2 to 8 times lower than for active copepods (Almeda, van Someren Gréve, and Kiørboe, 2017). We thus implement this lowered preference for passive feeders in the predation terms, and assume that the preference for passive feeders is $1/5$ the one of active feeders.

2.3 From individuals to populations

We use two representations of copepod population structure (Fig. 1b): a normalized number size spectrum $N(m)$ (in # L^{-1} µgC^{-1}, see Appendix F.1 for definitions) and a discrete stage structure C_s (µgC L^{-1}), where s indicates a size-range, derived as an approximation of the continuous size spectrum. The continuous size spectrum is used for analytical solutions and the stage structured model is used for dynamic simulations. The stage structured model is derived from the continuous

formulation in Appendix F.

The stage-structured formulation divides the biomass in size classes $s \in [1:S]$:

$$C_s = \int_{m_{s-1}^+}^{m_s^+} N(m) m \, \mathrm{d}m, \tag{8}$$

where $N(m)$ is the number spectrum (# L^{-1} µgC^{-1}) and m_s^+ is the upper size limit of the size class. The biomass in the adult stage is $C_S = N_\mathrm{a} m_a$, due to the adult stage being discrete in the continuous formulation. Each size class is represented by the geometric mean of the size class' mass range: $m_s = \sqrt{m_{s-1}^+ m_s^+}$. The numerical approximation assumes that the biomass production and mortality are constant within the size class. We can write general dynamic equations for the size classes and the adult stage as:

$$\frac{\mathrm{d}C_1}{\mathrm{d}t} = \overbrace{bC_S}^{\text{Births}} + \overbrace{g_1 C_1}^{\text{Biomass accumulation}} - \overbrace{\gamma_1 C_1}^{\text{Somatic growth}} - \overbrace{\mu_1 C_1}^{\text{Losses}}, \quad \text{for } s = 1 \tag{9}$$

$$\frac{\mathrm{d}C_s}{\mathrm{d}t} = \gamma_{s-1} C_{s-1} + g_s C_s - \gamma_s C_s - \mu_s C_s, \quad \text{for } 2 \leq s < S \tag{10}$$

$$\frac{\mathrm{d}C_S}{\mathrm{d}t} = \gamma_{S-1} C_{S-1} - \mu_S C_S, \quad \text{for } s = S \tag{11}$$

where b is the birth rate (Eq. 7). The factor γ_s (d^{-1}) describes the transfer of biomass between size classes, i.e. describes somatic growth. This rate is derived based on equilibrium conditions (de Roos et al., 2008):

$$\gamma_s = \frac{g_s - \mu_s}{1 - (\frac{m_{s-1}^+}{m_s^+})^{1-\mu_s/g_s}}, \tag{12}$$

and depends on the net energy gain, mortality and m_{s-1}^+/m_s^+: the ratio between the lower and upper mass boundaries of the size class.

2.4 From populations to the community

The copepod community is represented by a number I of populations. Each population i is characterized by the traits adult mass $m_{\mathrm{a},i}$ and feeding mode $\omega_{\mathrm{a},i}$. It is between individuals of the community that food-encounter and predation occurs. Thus, below we describe the available and encountered food for each stage s, which is required to calculate the feeding level (Eq. 1) and predation mortality of the copepods.

2.4.1 Encountered food

We assume that all organisms consume prey following a log-normal size preference function (Ursin, 1973; Hansen, Bjornsen, and Hansen, 1994). A predator of size m prefers prey (m_{py}) of size:

$$\phi(m_{\mathrm{py}}, m) = \exp\left[-\frac{\left(\ln\left(\frac{\beta m_{\mathrm{py}}}{m}\right)\right)^2}{2\sigma^2}\right], \tag{13}$$

where β is the preferred predator:prey mass ratio, and σ the standard deviation. As the size classes span a range of sizes, we use an integrated measure of the preferences, derived by integrating equation 13 across each size class, to form $\Phi(m_{\mathrm{py}}, m)$ (Appendix G).

Copepods can eat protists P (µgC L^{-1}), other (smaller) copepods of the same or of different populations, and fecal pellets F (µgC L^{-1}) (coprophagy). Food available $E(m)$ (µgC L^{-1}) equals the product of the preference function and the biomass of each corresponding prey size-group:

$$E(m) = \underbrace{\sum_{i=1}^{I}\sum_{s=1}^{S} c_{\mathrm{py}}\Phi(m_{i,s}, m)C_{i,s}}_{\text{Copepod prey}} + \underbrace{\sum_{k=1}^{K}\Phi(m_k, m)P_k}_{\text{Protist prey}} + \underbrace{\sum_{l=1}^{L}\Phi(m_l, m)F_l}_{\text{Fecal pellets}}. \tag{14}$$

where c_{py} is the function that lowers the preference for small passive feeders (eq. E.2).

2.4.2 Copepod losses

Mortality μ (d^{-1}) of copepods consists of predation μ_{pr}, starvation μ_{s} (Eq. 6) and mortality due to predation by higher trophic levels μ_{htl}, i.e., organisms larger than the largest copepods explicitly considered in the model (e.g. fish).

Predation rate on copepods of size m_{py} is the sum of food ingested by all predators weighted by the fraction that the prey $C_{\mathrm{py},s}$ represents to the total food eaten by each predator. To obtain the carbon-specific rate we divide by the biomass of prey ($C_{\mathrm{py},s}$). Hence, the terms cancel out and predation mortality rate (d^{-1}) becomes:

$$\mu_{\mathrm{pr}}(m_{\mathrm{py}}) = \sum_{i}^{I}\sum_{s}^{S}\frac{c_{\mathrm{py}}\Phi(m_{\mathrm{py}}, m_{i,s})}{E_{i,s}} h m_{i,s}^{n} f_{\omega,i}(m_{i,s})C_{i,s}, \tag{15}$$

where c_{py} is the lowered preference for small passives (Eq. E.2).

The mortality by higher trophic levels $\mu_{\mathrm{htl}}(m)$ (d^{-1}) acts as a closure term on the entire model. We expect a higher mortality pressure in environments with high productivity and higher biomass.

Therefore, we use a mortality term that increases with biomass within the community and within each population (used in Record, Pershing, and Maps, 2013):

$$\mu_{\text{htl}}(m) = p_{\text{htl}}(m)\frac{\mu_{\text{htl.0}}}{m_s^+/m_{s-1}^+}m^{-1/4}C_{i,s}^{(\Gamma)}B(m)^{(1-\Gamma)}, \tag{16}$$

where $\mu_{\text{htl.0}}$ is the coefficient (µgC$^{1/4}$ µgC^{-2} L^{-2} d^{-1}), which we divide by the ratio of the boundaries (m_s^+/m_{s-1}^+) of each size class to correct for the number of size classes. $p_{\text{htl}}(m)$ is a sigmoidal function used to impose the mortality only on the largest size classes (see eq. B.2 and fig. B.1). This mortality is imposed on copepods with a size larger than $m_{\text{htl}} = m_{\max}/\beta$ (where $m_{\max}$ is the size of the largest copepod in the community) and declines with mass $\propto m^{-1/4}$; since the mortality on the smaller sized organisms is already explicitly represented in the model. Γ imposes the preference of predators for specific populations/stages or for whole size range intervals B. If $\Gamma = 1$, the density dependence is imposed on each stage of each populations ($C_{i,s}$), if $\Gamma = 0$ the density-dependence is imposed on the biomass (B) within the size ranges. We chose $\Gamma = 0.2$ (Appendix B). The biomass B represents all copepods in the size range $[m/10^{\sigma_F/2} : m10^{\sigma_F/2}]$, where σ_F is the width of the predation function of a predator and is equivalent to 1. The biomass then becomes:

$$B(m) = \sum_i \sum_s C_{i,s}(m_{i.s}/10^{\sigma_F/2} < m \leq m_{i.s}10^{\sigma_F/2}). \tag{17}$$

2.5 Size-based protist model

Protists are described by an unstructured model (Ward and Follows, 2016) with K size classes. Each size class k is characterized by the geometric mean of the body-mass m_k within the size-range. The dynamics of the biomass concentration in each group P_k (µgC L^{-1}) is driven by the net energy gain $\nu_k(m)$ which represents the division rate (d^{-1}), and losses μ_k (d^{-1}) due to predation mortality and other causes:

$$\frac{\mathrm{d}P_k}{\mathrm{d}t} = \underbrace{\nu_k P_k}_{\text{Division rate}} - \underbrace{\mu_k P_k}_{\text{Total mortality}} . \tag{18}$$

2.5.1 Protist growth

All protists are potential mixotrophs that acquire resources through a mix of photo(auto)trophy and phagotrophy (eating other organisms). Hence protists simultaneously perform photosynthesis, take

up nutrients, and predate on smaller organisms. Uptake rates follow a type 2 functional response. The uptake rate η_X (d^{-1}) of a resource (X), which can either be light L_{PAR} (µE s^{-1} m^{-2}), nitrogen N (µgN L^{-1}), or food E_{u} (µgC L^{-1}), by a protist of size m is:

$$\eta_{\mathrm{X}}(m) = \overbrace{\psi_X(m)}^{\text{Maximum uptake rate}} \frac{\alpha_X(m)X}{\alpha_X(m)X + \psi_X(m)}, \tag{19}$$

where $\psi_X(m)$ represents the maximum uptake rate of the resource X (d^{-1}) and α_X is the affinity for resource X. The affinities for uptakes, α_{X} are determined by allometric scalings with exponents $-1/3$, $-2/3$, and $-1/4$ for light, nitrogen, and food respectively (see Appendix B.2 for detailed description and parameter values). The uptake of nutrients is measured in the equivalent units of carbon by assuming a fixed C:N ratio of the cells. The uptake of food is based on the same size preference function as for copepods (Eq. 13 with different parameters; see Appendix B.2):

$$E_{\mathrm{u}}(m) = \sum_{k=1}^{K} \Phi(m_k, m) P_k. \tag{20}$$

Protists may be limited by either carbon or nitrogen. We represent this by imposing Leibig's law on the total carbon gains ($\eta_{\mathrm{L}} + \eta_{\mathrm{E}} - \eta_{\mathrm{R}}$), where the respiration rate η_{R} (d^{-1}) is imposed, and nitrogen gains ($\eta_{\mathrm{N}} + \eta_{\mathrm{E}}$). Hence, the division rate of cells is (d^{-1}):

$$\nu_{\mathrm{u}}(m) = \min\left[\eta_{\mathrm{L}}(m) + \eta_{\mathrm{E}}(m) - \eta_{\mathrm{R}}(m),\ \eta_{\mathrm{N}}(m) + \eta_{\mathrm{E}}(m)\right], \tag{21}$$

Note that food ingestion η_{E} enters in both the carbon and the nitrogen budgets. Surplus of nitrogen is leaked back to the environment at a rate (d^{-1}):

$$\eta_{\mathrm{leaks}} = \max[0,\ \eta_{\mathrm{N}}(m) - \eta_{\mathrm{L}}(m) + \eta_{\mathrm{R}}(m)]. \tag{22}$$

2.5.2 Protist losses

Total mortality rate of protists μ_{u} (d^{-1}) is the sum of predation mortality ($\mu_{\mathrm{u,pr}}$) and background mortality ($\mu_{\mathrm{u,b}}$). Protist mortality rate is the sum of all the predation terms imposed by all copepods and protists on the given prey size class (following the same logic as in equation 15):

$$\mu_{\mathrm{u,pr},k} = \sum_{i=1}^{I} \sum_{s}^{S} \frac{\Phi(m_k, m_{i,s})}{E_{i,s}} h m_{i,s}^{n} f_{i,s} C_{i,s} + \sum_{j=1}^{K} \frac{\Phi(m_k, m_j)}{E_{u,j}} \eta_{\mathrm{E},j} P_j. \tag{23}$$

The background mortality $\mu_{u,\mathrm{b}}$ (d^{-1}) mainly represents viral lysis. We assume that it increases with biomass and decreases with cell size as:

$$\mu_{\mathrm{u,b},k} = \frac{\mu_{\mathrm{u,b0}(m)}}{m_k^+ / m_{k-1}^+} P_k, \tag{24}$$

where $\mu_{\mathrm{u,b0}}(m)$ is the strength of the mortality. Making the mortality inversely proportional to the ratio of the boundaries of each protist size class (m_k^+ / m_{k-1}^+) ensures that the strength of this linear mortality remains the same if the number of size classes is changed.

2.6 Parametrization and temperature dependencies

All copepod parameters can be found in table 1 and a detailed explanation of all parameters derivation can be found in Appendix B. Effects of temperature on physical and physiological processes are implemented as factors on the relevant parameters of copepods and protists. We use the Q_{10} factor to model the effects of temperature on each corresponding parameter, which for a given rate R is:

$$R = R_{\mathrm{ref}} Q_{10}^{(T - T_{\mathrm{ref}})/10}, \tag{25}$$

Where T is the temperature, T_{ref} the reference temperature and R_{ref} the rate at the reference temperature. We use $Q_{10} = 2$ for the following physiological processes: maximum ingestion rate of copepods, maximum uptake rates of protists and respiration rates. The parameters affecting the affinities α_X of protists are determined by chemical and physical processes (Serra-Pompei et al., 2019): For uptake of light we use $Q_{10} = 1$, as photosynthesis is a photochemical process independent of temperature. For uptake of nitrogen a $Q_{10} = 1.5$ is roughly the temperature scaling of diffusion of nutrients towards the cell. It is unknown whether the clearance rate of protists and copepods is temperature dependent. Swimming speed might increase, but so would the swimming speed of prey and the escape rate. We assume a $Q_{10} = 1.5$, which is the approximate temperature dependence for the seawater viscosity and would account for changes in swimming speed. Background mortality and mortality by higher trophic levels are assumed to have a $Q_{10} = 2$. Reference temperature for all parameters was of 15°C (except for the maximum uptake rates of protists, which was of 18°C), in accordance to the data from which they were derived.

2.7 Bio-geochemical dynamics

The protist (unicellular) and copepod (multicellular) models are embedded in a simple bio-geochemical model that describes the dynamics of light, nutrients and vertical exchange with a deep layer with constant nutrient concentration (fig. 1d). The integated model also includes a representation of copepod fecal pellets. We use a simple physical model, similar to that used in Evans and Parslow (1985) that assumes a surface mixed layer of depth $z(t)$ where all biological interactions occur. The concentration of organisms and particles is homogeneous over the mixed layer. Below the mixed layer, state variables are not resolved, hence processes such as deep chlorophyll maxima cannot be represented. The model then becomes a simple semi-chemostat model with a mixing rate (ρ) between the two layers (Evans and Parslow, 1985; Anderson, Gentleman, and Yool, 2015).

2.7.1 Nitrogen

Nitrogen is mixed between the upper mixed layer and the deep layer at a rate ρ (d^{-1}). The concentration in the deep layer is N_0 (µgN L^{-1}). Other sources of nitrogen are the remineralization r of the fecal pellets F_k (d^{-1}) and remineralization of a fraction δ of the background losses of copepods and protists. Finally, nitrogen is taken up by protists η_N (d^{-1}), and in case of excess nitrogen, leaked back to the environment η_leaks (d^{-1}):

$$\frac{\mathrm{d}N}{\mathrm{d}t} = \underbrace{\rho(N_0 - N)}_{\text{Exchange with deep layer}} + \frac{1}{Q_\mathrm{C:N}}\Bigg[\underbrace{r\sum_l^L F_l}_{\text{Remin. fecal pellets}} + \underbrace{\sum_k^K (\eta_{\mathrm{leaks},k} - \eta_{\mathrm{N},k})P_k}_{\text{Leaks and uptake by protists}} \tag{26}$$

$$+ \underbrace{\delta\Big(\sum_k^K \mu_{\mathrm{b,u},k}P_k + \sum_i^I\sum_s^S \mu_{\mathrm{b},s}C_{i,s}\Big)}_{\text{remineralization of dead matter}} + \underbrace{\sum_i^I\sum_s^S \eta_{\mathrm{DON},s}C_{i,s}\Big)}_{\text{N excretion by cops.}}\Bigg], \tag{27}$$

where $Q_\mathrm{C:N}$ is the C:N ratio, which we assume to be constant. η_DON is the excretion of dissolved organic nitrogen by copepods. We assume this excretion to be equal to the metabolic costs and what is not invested into reproduction:

$$\eta_{DON} = \sum_i^I\sum_s^S \kappa m^p C_{i,s} + \sum_i^I (1-\epsilon_\mathrm{r})g(m_a)C_S. \tag{28}$$

2.7.2 Fecal pellets dynamics and carbon export

Fecal pellets are produced by copepods at a rate f_{pp} (d^{-1}) from the non-assimilated food:

$$f_{\mathrm{pp}}(m) = (1-\epsilon) h m^n f(m). \tag{29}$$

The sinking rates of fecal pellets are strongly defined by their size (Small, Fowler, and Ünlü, 1979), and the size of each fecal pellet is proportional to the size of the producer (Mauchline, 1998). Hence, we group the fecal pellets in L size groups characterized by the (geometric) mean carbon-mass m_l for each size group. The biomass dynamics in each size-group of fecal pellets F_l (μgC L^{-1}) in the water column is:

$$\frac{\mathrm{d}F_l}{\mathrm{d}t} = \underbrace{\sum_i^I \sum_s^S f_{\mathrm{pp}}(m_{i,s}) C_{i,s}}_{\text{Total fecal pellet production}} - \underbrace{r F_l}_{\text{Remin.}} - \underbrace{\frac{v_{\mathrm{s}}(m_l)}{z} F_l}_{\text{Sinking}} - \underbrace{\mu_{\mathrm{p,f},l} F_l}_{\text{Consumption by copepods}}, \tag{30}$$

where r (d^{-1}) is the remineralisation rate, $v_{\mathrm{s}}(m_l)$ (m d^{-1}) is the sinking speed and z (m) is the thickness of the upper mixed layer. $\mu_{\mathrm{pr},l}$ (d^{-1}) is the consumption of fecal pellets by copepods:

$$\mu_{\mathrm{pr,f},l} = \sum_i^I \sum_s^S \frac{\Phi(m_l, m_{i,s})}{E} h m_{is,}^n f(m_{i,s}) C_{i,s}. \tag{31}$$

2.7.3 Physical forcing

We use the model to simulate two scenarios: a stable environment with constant environmental forcing over time, and a seasonal environment. The environmental forcings are light in terms of photosynthetically active radiation (L_{PAR} in µE s^{-1} m^{-2}), the mixing rate of nitrogen in the system ρ (d^{-1}) and temperature T (°C). We use the stable scenario to explore the response of the model under varying environmental conditions.

The seasonal scenario uses time-dependent forcing (Anderson, Gentleman, and Yool, 2015), previously used in Evans and Parslow (1985) and Fasham, Ducklow, and McKelvie (1990), including a changing thickness of the mixed layer $z(t)$ (details in Appendix C).

In the seasonal environment, to allow protists and copepods to emerge again every year after winter, we add a small background concentration that is governed by chemostat dynamics in the

equation for the first copepod stage (eq. 9) and in the protist equations (eq. 21):

$$\rho_{\text{seed}}(B_{\text{seed}} - B_{\text{c/p}}). \tag{32}$$

$B_{\text{c/p}}$ is the biomass of nauplia or protists and ρ_{seed} is the input rate. We made ρ_{seed} proportional to the maximum ingestion rate of each size-group to avoid it strongly affecting the dynamics of the group. B_{seed} has the form of a normalised biomass spectrum (i.e. we corrected for the size width of each bin) and is also at a concentration low enough as not to affect the general dynamics.

2.8 Numerical implementation

In the model, active adult copepods size can range from 0.2 µgC to 1000 µgC, and passive copepods from 0.2 µgC to 5 µgC (the same size ranges can be imposed assuming the swimming penalty on large passive feeders from Appendix E). We simulate $I = 8 + 3$ copepod populations: 8 populations of active feeders and 3 populations of passive feeders. This number of populations corresponds to at least two populations of each feeding mode per log-interval within the size range. Each copepod population was discretised in $S = 8$ size-intervals (1 adult stage and 7 juvenile size-intervals). We performed a sensitivity analysis on the number of size-intervals (Appendix D, fig. D.1 and D.2): results were substantially different for populations with less than 5 size classes. Above 5 size classes, biomass converged. Protists range from 10^{-7} µgC to 10^{-1} µgC with $K = 14$ size groups. The size range of fecal pellets was converted from the minimum and maximum size of copepods (the smallest juveniles and the largest adult) using the conversions in Appendix B. The number of fecal pellets size bins is $L = 3$ in the steady environment and $L = 10$ in the seasonal scenario. The model was solved in MATLAB and the code can be found in https://github.com/cam-sp/Copepod_sizebased_model.

The scenario with a constant environmental forcing was run for 20000 days, whereas the seasonal scenario for 50 years, enough to converge into a steady solution. Initial conditions were the same for all the runs, of 1 µgN L^{-1} for the nitrogen pool, 5 µgC L^{-1} for each protist size class, 5 µgC L^{-1} for each copepod size class, and 0 µgC L^{-1} for fecal pellets. For the parameter sweep plot (simplified bifurcation diagrams, fig. 6), we varied the value of the input of nitrogen in the system (ρ) from 10^{-3} d^{-1} to 10^{-1} d^{-1} in 80 steps (each corresponding to a model run of 20000 days, all with the same initial conditions as stated above). We then took the average, maximum and minimum values for the last 5000 days of each run, time at which the model had converged into a stable solution. In this same plot, we only show the populations for which the final averaged reproductive rate is positive or

Symbol	Description	Units	Value	
			Active	Passive
m	Body mass copepods	µgC $\#^{-1}$		
m_{a}	Body mass adult copepods	µgC $\#^{-1}$		
m_0	Offspring mass	µgC $\#^{-1}$		
$z_{\mathrm{a:o}}$	Adult to offspring mass ratio	-	100	
m_{py}	Body mass of a prey	µgC $\#^{-1}$		
β	Preferred predator:prey mass ratio	-	10000	100
σ	Width of prey-size function	-	1.5	1
v	Clearance rate coefficient	L µgC$^{-3/4}$ d^{-1}	0.011	0.0052
q	Clearance rate exponent	-	$-1/4$	
h	Maximum ingestion rate coefficient	µgC$^{1/4}$ d^{-1}	1.37	0.4
n	Maximum ingestion rate exponent	-	$-1/4$	
κ	Respiration rate coefficient	µgC$^{1/4}$ d^{-1}	0.16	0.048
p	Respiration rate exponent	-	$-1/4$	
ϵ	Assimilation efficiency	-	0.67	
ϵ	Reproduction efficiency	-	0.25	
c_{py}	Reduced preference for passives	-	1	1/5
$\mu_{\mathrm{htl.0}}$	Mortality by higher trophic levels coefficient	µgC$^{1/4}$ µgC^{-2} L^{-2} d^{-1}	$0.003 \times h$	
$Q_{\mathrm{C:N}}$	Carbon to nitrogen ratio	-	5.6	
σ_{htl}	Width of the prey-size function for a higher trophic level	-	1	

Table 1. Copepod variables and parameters. # refers to "numbers" and units of $\#^{-1}$ are "per individual". The rest of parameters and corresponding derivation are explained in Appendix B.

the biomass spectrum of all stages within a population are above 10^{-40} µgC L^{-1} µgC^{-1}. These latter conditions are relevant when productivity is very low and the model takes too long to converge.

2.9 Analytical solutions

We developed analytical solutions of the copepod model for the community and population size spectra, size at age, development time from nauplii to adult copepod, and the maximum population growth rate (Appendix F). These analytical solutions assume a constant, size-independent feeding level $f(m) = f_0$. The feeding level determines the growth rate, the reproduction rate, and the predation rate. Knowing growth (from eq. F.5) and mortality we can solve the McKendric-von Foerster

equation (eq. F.2) for the size spectrum of a copepod population and find the population growth rates. Repeating this exercise for a range of copepod populations leads to results for the total copepod community.

Without density dependent effects, a population will grow at its maximum rate $r_{\max}$ (chapter 7 in Andersen, 2019):

$$r_{\max} = A m_{\mathrm{a}}^{n} \frac{n}{z_{\mathrm{a:o}}^{n} - 1} \left[(1-a) \ln(z_{\mathrm{a:o}}) + \ln\left(\frac{\epsilon_r}{a}\right) \right], \tag{33}$$

where $z_{\mathrm{a:o}} = m_a/m_0$ represents the mass ratio between adults and nauplii, $A = \epsilon h (f_0 - f_{\mathrm{c}})$ is the coefficient of the growth rate of individuals (Appendix F.5), and a is the physiological mortality, which is the ratio between mortality and growth rate (eq. F.15). Equation 33 shows that the population growth rate increases with the growth rate coefficient A and decreases with adult size with exponent $-1/4$. The term in the brackets is a correction factor that decreases as the reproductive efficiency ϵ_{r} decreases and the physiological mortality a increases, i.e., if either the mortality increases and/or the growth decreases.

3 Results

We first present the results of the analytical approximations. Then we show full dynamic simulations of the entire model complex in the constant environment for various nutrient inputs. Finally we show an example of a seasonal scenario in a temperate system.

3.1 Analytical solutions

3.1.1 Development rates

Large copepods develop at a slower pace than small copepods, and passive feeders have longer development times than active feeders (fig. 3). Development times from birth to maturity are of the same order of magnitude as observed development times at saturating food concentrations. However the slopes differ, where the model predicts an increasing development time with size following the allometric scaling of parameters, whereas observations are rather constant with size. Development time increases as the feeding level decreases, since less food results in lower growth rates and longer development times. The lower feeding level shown in the figure, $f_0 = 0.3$, is around the feeding level that emerges from the dynamic simulations.

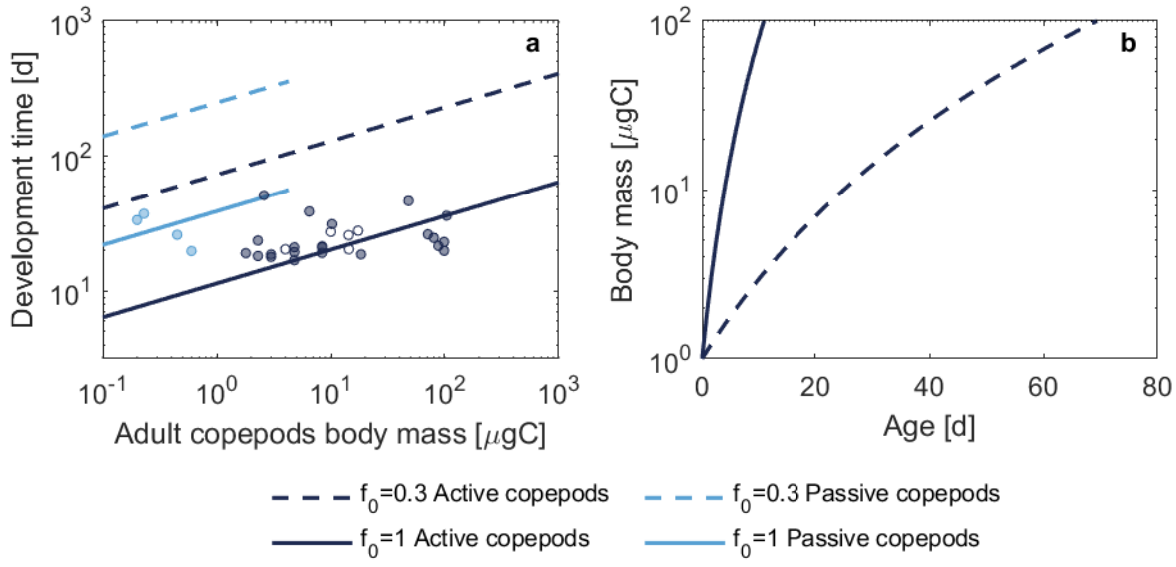

Fig. 3. Development time from birth to maturity (**a**) and size-at-age (**b**) for active and passive feeders (dark and light blue respectively, empty dots are mixed feeding copepods) at a saturating feeding level $f_0 = 1$ (solid) and at a low feeding level $f_0 = 0.3$ (dashed). Dots are data from Kiørboe and Sabatini (1995) (table in Appendix 1 of that paper) at saturating food conditions. The feeding mode of copepod species from the data were determined using the data-set of Brun, Payne, and Kiørboe (2016b). **b**, Size-at-age for a population of active feeding copepods with adult size $m_\mathrm{a} = 100$ µgC (top of y-axi) and nauplii size $m_0 = 1$ µgC (bottom of y-axi).

3.1.2 Minimum food requirements and population growth rates

In a stable environment the most competitive organisms are those that persist at the lowest food concentrations (Tilman, 1982). A measure of this competitive ability is E^*, the concentration of food where the net gain $\nu(m) = 0$ (i.e. the feeding level equals the critical feeding level $f(m) = f_c(m)$). The best competitors are protists, since they have the lowest E^* (fig. A.1), followed by small passive feeders and finally large active feeders. The E^* refers to the competitive ability of a single organism at a given size, but copepods need to fulfill their life cycle for the population to persist. Thus, growth rates at the population level are needed.

The population growth rate indicates the competitive ability of a copepod population. Active copepods have higher population growth rates in high food environments (fig. 4). Passive copepods outcompete active copepods at low prey concentrations or at high mortality levels (fig. 4b+d). This is due to the lower metabolic rate and mortality of passive feeders. Active copepods dominate when

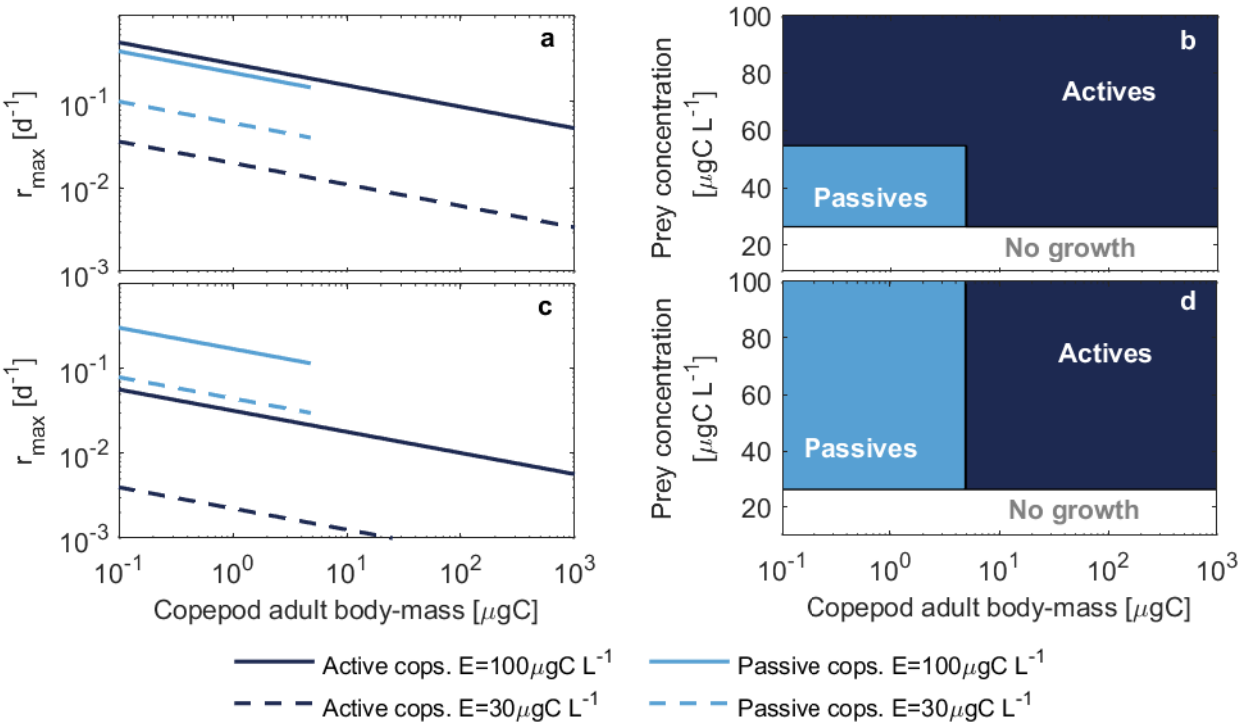

Fig. 4. Population growth rates with a low (**a,b**) physiological mortality ($a = 0.3$) and a high (**c,d**) physiological mortality ($a = 0.7$).(**a,c**) Maximum population growth rates $r_{\max}$ from the analytical approximation (eq. 33) as a function of adult size for high prey concentration ($E = 100$ µgC L^{-1}; solid lines) and low prey concentration ($E = 30$ µgC L^{-1}; dashed). (**b,d**) feeding mode with the highest $r_{\max}$ as a function of adult body-mass and prey concentration. Areas colored in dark blue indicate that active feeders win, areas in light blue that passive feeders win, areas in white show where copepods populations have negative growth. We assume a of passive feeders to be 1/5 the one of active feeders following eq. E.2. Prey concentration is a fixed value.

prey concentration is high due to their higher maximum ingestion rate. Overall, the calculations of $r_{\max}$ and E^* give similar predictions: small passive copepods dominate in environments with high mortality and/or low food, and active copepods dominate in environments with high food conditions.

Insights from the analytical solutions make it easier to interpret the more complex numerical solutions. However, one needs to be aware that the analytical approximations assume a constant feeding level and the same predator-prey mass ratio (β) between organisms of the same size. In the full model, the feeding level varies between size-classes and depends on the availability of food. Further, the predator-prey mass ratio differs between active copepods, passive copepods and protists,

and therefore organisms of the same size do not necessarily compete for the same prey. Moreover, considering the overlap between sizes of small juvenile copepods and protists, and corresponding β, competition between protists and small copepods seems possible. These potential feed-backs can only be accounted for with dynamic simulations.

3.2 Dynamic simulations

3.2.1 Constant environmental forcing

Results from numerical simulations match results obtained analytically. The biomass spectrum declines with size (Fig. 5). The Sheldon spectrum (mgC m^{-3}, see Appendix F.1 for definition) is flat (fig. H.1), in accordance with the predictions from the analytical approximation (fig. 5 dash-dotted lines, and Appendix F.5, fig. F.1). The Sheldon spectrum also shows an increase in total biomass in the system when the nitrogen input is higher (fig. H.1). Mortality declines with size (fig. 5e+f), as expected from the analytical approximation (Appendix F).

Dynamics in the system are dominated by competition for food, as can be seen from the relatively low feeding levels of copepods (fig. 5c,d). The feeding levels are on average around 0.3, slightly above the critical feeding level. This feeding level is lower than the one found in the analytical calculations, f between 0.4 and 0.83, based on a balance between growth and mortality (Appendix F.10). Within each copepod population, the size classes that are closest to starvation are the ones that dominate in terms of biomass, as it can be seen by their feeding levels close to the critical feeding level. This suggests bottlenecks, where biomass accumulates due to a slow growth in that size class. Populations with feeding levels below the critical level go extinct. Finally, note that the critical feeding level is constant across sizes, indicating that small copepods are not necessarily more susceptible to starvation than large copepods (if reserves are not accounted for).

Mortality is dominated by predation (fig. 5e,f). Predation mortality of small protists is imposed by large protists, while mortality of large protists originates from copepod predation. Small copepods and the juveniles of most copepods are strongly preyed-on by large copepods, whose populations are more numerous at higher levels of nitrogen inputs (fig. 5b,d,f). Overall, higher nutrient inputs lead to the emergence of larger active copepods, resulting in a high predation pressure on small copepods.

The response of the community to the entire range of nutrient inputs is explored in Fig. 6. The first copepods that can persist are small passives and large active feeders. The persistence of a large

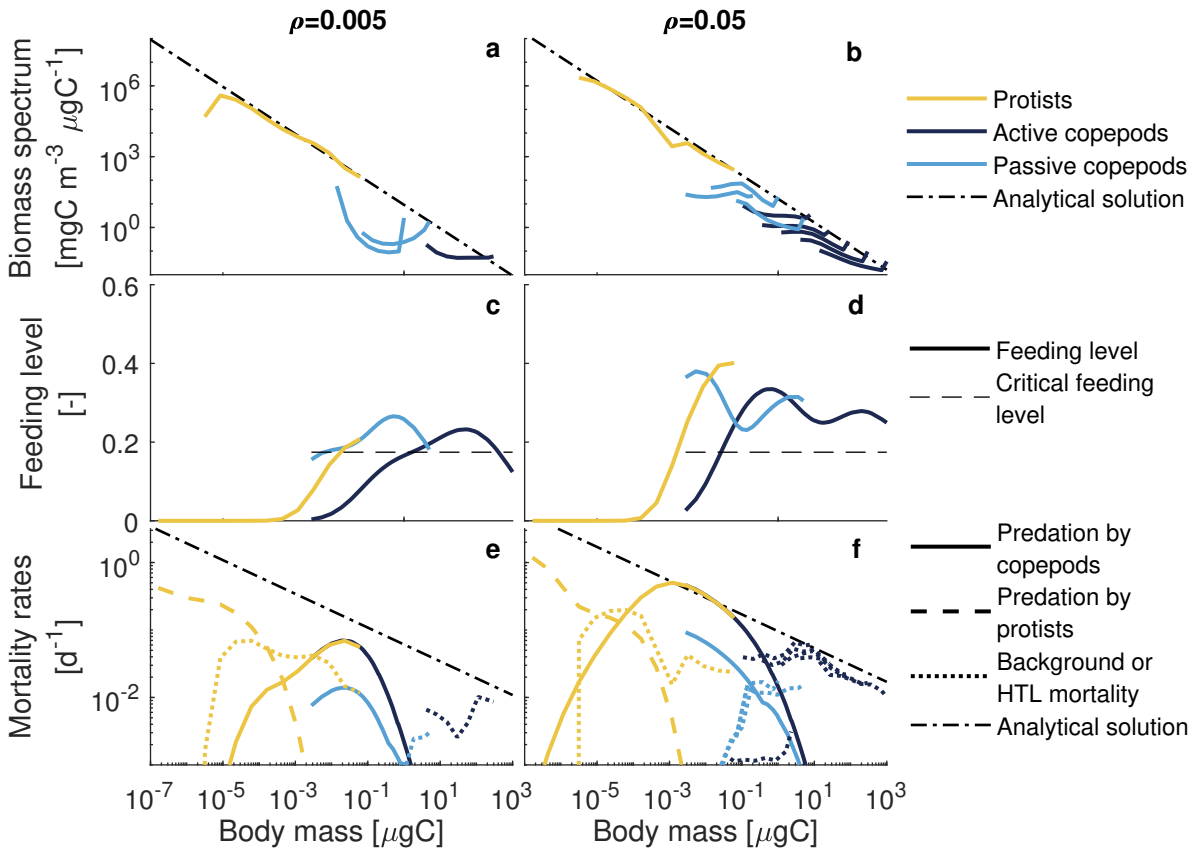

Fig. 5. Results from numerical simulations under low and high input of nitrogen (left column $\rho = 0.005$ d^{-1} and right column $\rho = 0.05$ d^{-1}). All panels show protists (yellow), and passive/active copepods (dark/light blue), with predictions from the analytical approximations (black dash-dotted lines). (**a,b**) Biomass spectrum (see Appendix F.1). Each line segment of copepods represents a population. The copepod populations shown are those persisting at the end of the simulation. The adult stage is discrete and therefore for this plot we assumed its bin width is the same as the size class just before the adult size. (**c,d**) Time-averaged feeding level f with dashed lines showing the critical feeding level f_c. Feeding levels that are below the critical feeding level show that organisms are starving, which prevents populations from surviving. (**e,f**) Mortality rate from predation by copepods (continuous lines), predation by protists (dashed), and background mortality for protists or mortality by higher trophic levels (HTL) for copepods (dotted lines). Starvation mortality is not shown as it can be identified from the feeding level panels. In both runs temperature was 15 C°, light $L_{\mathrm{PAR}} = 100$ µE s^{-1} m^{-2}, deep nutrients $N_0 = 140$ µgN L^{-1}, and mixed layer depth 10 m.

active feeder at low levels of productivity is at odds with the results found analytically (Figs. A.1 and 4). This large active can persist because it shares the prey field with the small passive feeder (due to the different predator-prey mass ratios, β), but it imposes predation on the juveniles of the

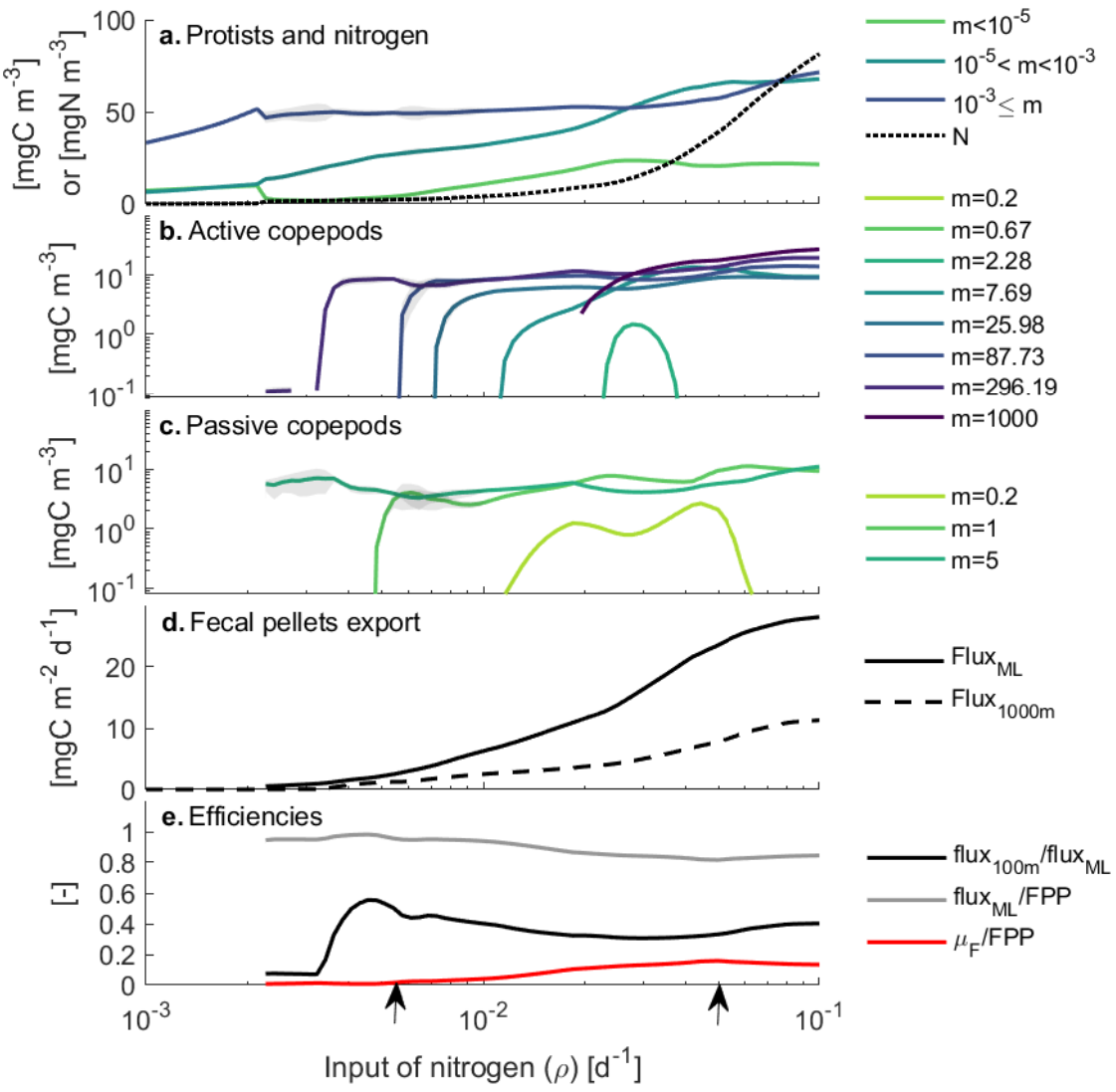

Fig. 6. Model output as a function of nitrogen input rate ρ. (**a**, **b** and **c**) Biomass averaged after model convergence. (**a**) Nitrogen (dotted) and protists grouped in cell-mass ranges (solid). (**b,c**) Biomass of adult active and passive copepods respectively. Shaded areas around the lines show maximum and minimum biomass values when the system oscillates. (**d**) Flux of fecal pellets out of the mixed layer (continuous) and at 1000 m (dashed, calculations in Appendix B). (**e**) Fraction of fecal pellets out of the mixed layer exported to a 1000 m (black), fraction of fecal pellets exported out of the mixed layer relative to fecal pellets production rate within the mixed layer (grey), and fraction of fecal pellets consumed relative to the fecal pellets production rate (red). Arrows at the bottom show the values of ρ where the runs of figure 5 were done. In all the runs temperature is 15 C°, light $L_{\mathrm{PAR}=100}$ µE s^{-1} m^{-2}, $N_0 = 140$ µgN L^{-1} and a mixed layer depth of 10 m.

passive feeders, indicating the presence of intraguild predation (Polis, Myers, and Holt, 1989). On the other hand, small active feeders never emerge in the system. In addition to the high predation by

large copepods, small active feeders are always starving (fig. 5c,d). This starvation originates from the competition of small active copepods with protists, where small active copepods are the losers.

Higher nutrient inputs lead to a greater coexistence of copepod populations. This is due to the density-dependent closure term which imposes a top-down control on the dominant populations, allowing the least competitive populations to emerge as productivity increases. Biomass of small passive feeders decreases at high levels of nitrogen inputs ($\rho > 0.05$ d^{-1}, fig. 6). This time, passive feeders are affected by the competition with intermediate active copepods (adults between 1 and 10 µgC) and the predation by adult copepods, showing again the presence of intraguild predation in the system.

Total biomass in the system increases with nitrogen inputs (fig. 6). First, biomass of protists increases, until top-down control by copepods is imposed. The copepod biomass increases by increasing the coexistence of copepod populations. Finally, total biomass in the system stops increasing. This is due to the density-dependent closure terms on copepods and protists (background mortality and mortality by higher trophic levels). This "top-down control" is reflected in the constant increase of N in the system at high levels of N inputs. All in all, the higher the productivity in the system, the higher the total biomass and the stronger the coexistence of copepod populations.

Total fecal pellets export increases with the nutrient input (fig. 6d). The higher export is a reflection of the higher copepod biomass. The fraction of fecal pellets that reaches 1000 m (the transfer efficiency) is lowest when small copepods dominate relative to large copepods ($\rho \sim 0.003$. fig. 6e). Once large copepod are established in the system the transfer efficiency becomes high (above 0.5) but decreases as populations of small copepods appear. This decrease in transfer efficiency is due to the slower sinking rates of fecal pellets from small copepods. On the other hand, the fraction of fecal pellets exported out of the mixed layer relative to the fecal pellets production is controlled by the consumption of fecal pellets by copepods (fig. 6e). Here copepods can consume up to 20% of the fecal pellets produced. Thus, the higher the copepod biomass, the higher the consumption of fecal pellets, and the stronger the attenuation of carbon flux out of the mixed layer.

3.2.2 Sensitivity analysis

The main results from the sensitivity analysis (Appendix D) are that predator-prey mass ratios (β) affect the size distribution within the copepod community. Small β favour small and intermediate copepods whereas large β favour large copepods (fig. D.3). A small width (σ) of the preference func-

tion removes copepods from the system (fig. D.4). Finally, variations in the assimilation efficiency for all copepods mainly affects the fecal pellets flux (fig. D.5). Intermediate assimilation efficiencies ($\epsilon = 0.5$) result in the highest carbon flux, as copepods have enough energy to grow but most of the food is excreted in the form of fecal pellets.

3.2.3 Seasonal scenario

The seasonal scenario, simulating a temperate ecosystem, has a marked spring bloom of protists (fig. 7a). The bloom is terminated partly by nitrogen depletion and partly by the predation of protists and copepods (figs. 7a and H.3). Total copepod biomass peaks in summer and autumn. The delay between the protists peak and the copepods peak is due to the development time of copepods. When food is plentiful during the spring bloom, copepods have the potential to reproduce, leading to a peak in specific reproduction rate (figs. 7e in grey and H.2). Despite this high specific reproductive rate, the total number of adult copepods is too low to produce a large total number of offspring. So, only when the new cohort of these offspring reaches adulthood (fig. 7c) and individuals reproduce again, can copepods significantly increase their numbers (see differences between specific (grey) and total reproductive rates in figs. 7e and H.2 and the peaks in biomass in figures 7). Hence, since the number of adults in spring is still too low due to starvation during the winter months, copepod biomass does not directly follow protists biomass.

The dominance of a population at a given time is a combination between food availability and predation. Reproduction occurs when there is enough food for adults, which is during most months of the year except in winter. Predation on small juvenile copepods occurs in summer and autumn, when large copepods are present. This predation can affect the development of cohorts. For example, some small active copepods have a high specific reproductive rate (fig. H.2) in summer and autumn, yet they do not manage to increase their biomass (fig. 7b) due to the high predation pressure (fig. 7). Finally, the smallest active copepods starve most of the time (fig. H.4) due to the lack of their prey (the smallest protists). Altogether, the passive-feeding strategy is favoured for small copepods.

There are two peaks in fecal pellet export, one in summer and another in autumn (fig. 7f). These peaks in export follow the dynamics of copepods biomass. Transfer efficiency of fecal pellets to a 1000 m varies between 0.35 and 0.55 and is mainly linked to the dynamics of the mixed layer. The transfer efficiency is highest when the mixed layer is deep (fig. H.5), which reduces the sinking distance and time between the depth of the mixed layer and a 1000 m. Copepod size does not seem

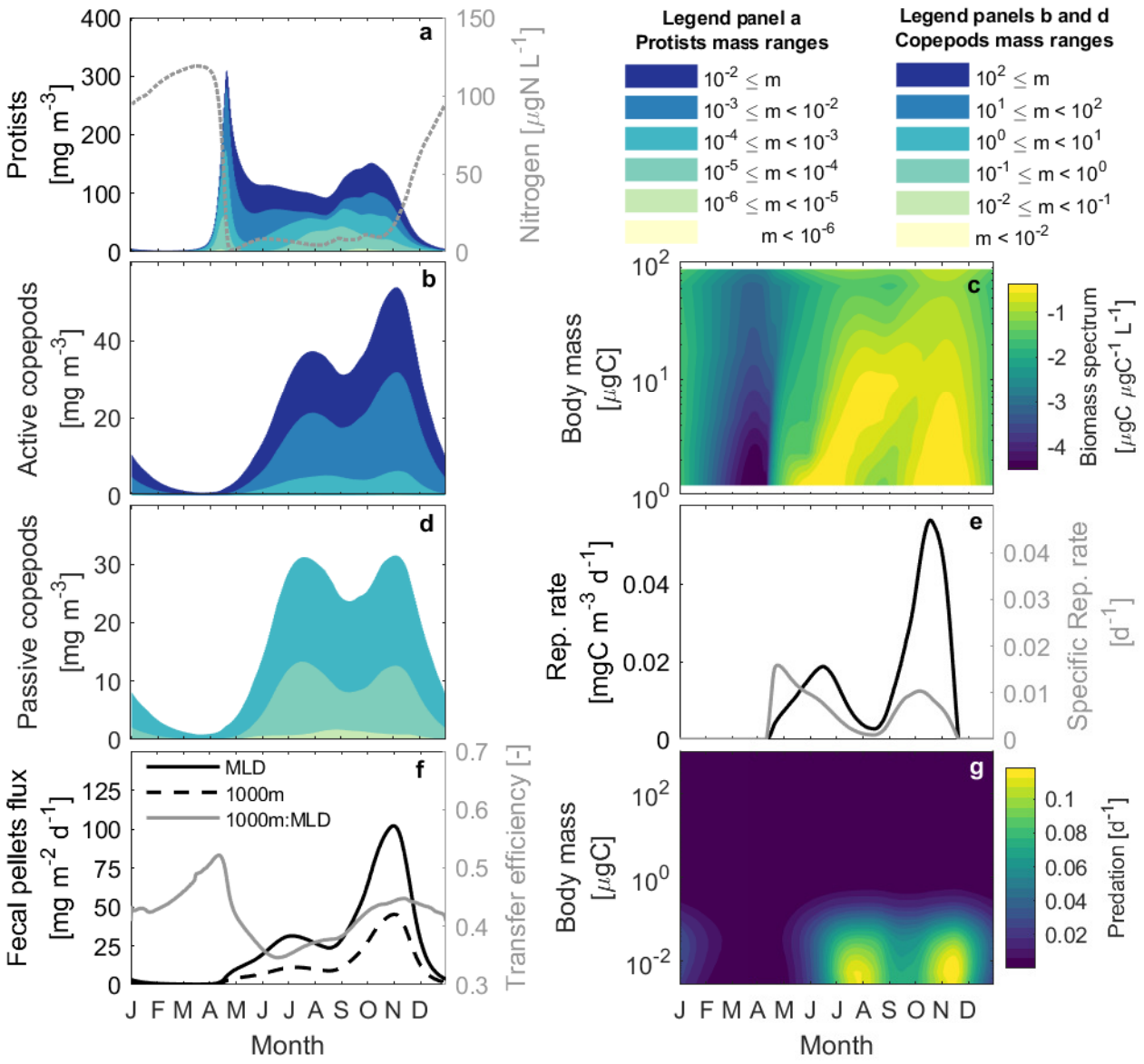

Fig. 7. Seasonal scenario. (**a**, **b** and **d**) Biomass concentration in upper mixed layer of protists (**a**), active copepods (**b**), and passive copepods (**d**), grouped into size ranges (see legends). For copepods, each size group contains juveniles and adults of all populations. (**a**) right *y*-axis: Nitrogen concentration within the mixed layer. (**c**) Cohort of an active feeding copepod population with an adult body-mass of 87 µgC. (**e**) Reproduction rate (black, left *y*-axis) and mass-specific reproductive rate (grey, right *y*-axis) of the copepod population from panel **c**. (**f**) left *y*-axis: Flux of fecal pellets leaving the mixed layer (black) and at 1000 m (black dashed). (**f**) right *y*-axis: transfer efficiency, i.e fraction of fecal pellets leaving the mixed layer that reach 1000 m. (**g**) Predation mortality imposed by copepods on active copepods only (other mortalities in Fig. H.3).

to affect the transfer efficiency (fig. H.5). On the other hand, the fraction of fecal pellets exported relative to the fecal pellets produced depends on the mixed layer when copepod concentration is low and on consumption of pellets by copepods when copepods concentration is high (fig. H.5). Overall, the dynamics of fecal pellets export are complex and depend on several factors.

4 Discussion

4.1 NUM model concept

We have presented the Nutrients-Unicellular-Multicellular (NUM) paradigm to model planktonic communities. The community structure is described as a size- and trait-distribution with a community composition that changes depending on the environmental conditions. The multicellular component is based on copepods as the dominant multicellular planktonic group, however, the framework is generic and can be parameterised for other life histories, such as krill or arrow worms, with modest effort. The central process is predation by larger organisms on smaller organisms. Using cell/body size to describe trophic interactions avoids the need to *a priory* decide the trophic level of each organism. Thus, the topology of the food web is an emergent and dynamic property which impacts ecosystem functions such as total primary production, energy transfer from primary producers to higher trophic levels, and carbon export from dead organisms and fecal pellets.

The development of the multicellular component is based on earlier efforts to describe fish populations (Hartvig, Andersen, and Beyer, 2011) and populations of zooplankton. For instance, Record, Pershing, and Maps (2013) resolved copepod ontogeny and several adult sizes to model the entire copepod community. Their framework, however, modelled only the copepod community and omitted predator-prey feed-backs, which is key to properly describe the trophic transfer of energy in the community. Heneghan et al. (2016) developed a generic size-based model of zooplankton, valid for any kind of zooplankton, coupled to a fish model. While this model does resolve predator-prey interactions, it omits the explicit modelling of reproduction by zooplankton. Zooplankton therefore reproduce irrespective of food availability, which breaks the mass balance of the energy transfer. The NUM modelling framework includes the mass balance from both predator-prey interactions and reproduction.

4.2 Macroecological patterns

The model framework reproduces several macro-ecological observations and predictions. First, the biomass spectrum declines with body-mass and a flat Sheldon spectrum is found in log size-groups with size (figs. 5 and H.1), across the entire unicellular and multicellular community (Sheldon, Prakash, and Sutcliffe Jr, 1972; Boudreau and Dickie, 1992; Sprules and Barth, 2015). The combination of size-dependent predation and the allometric scaling of metabolism leads to an emergent mortality rate that is weakly declining with body mass, as also observed in nature (McGurk, 1986; Hirst and Kiørboe, 2002). These two patterns are predicted by both analytical and numerical models. The dynamical simulations further show that the food chain becomes longer as the productivity increases. These three patterns are relatively generic and tend to emerge from the assumptions of mass balancing and size-specific predation (Andersen and Beyer, 2006).

4.3 Traits distribution within the copepod community

Important patterns of copepod communities that are produced by the model (and discussed in the following sections) are: the community is a diverse assemblage of sizes and feeding modes and is not dominated by a single population. Small passive feeding copepods tend to dominate in low productivity systems and at high mortality levels. Small active feeding copepods are outcompeted by protists and suffer from high predation mortality by large copepods, which removes them from the system, favouring the passive feeding strategy. Active feeders are present in most sizes and productivity levels. Finally, the model reproduces qualitatively the seasonal succession of protists and copepods with a time lag in the response of the copepod populations.

4.3.1 Size

Copepod body size mainly depends on the predator-prey mass ratio, mortality and productivity. Copepod body-size correlates positively with the input of nitrogen to the system. This is observed in data from surface dwelling copepods (Brun, Payne, and Kiørboe, 2016a), where average copepod size in the community increases with the productivity of the system. However, one cannot directly compare the model and the data here, as the observations are driven by seasonal changes with latitude, where seasonal systems are expected to favour larger copepods (Sainmont et al., 2014). In the model, the largest copepods appear when food chains are longer (several heterotrophic protists and

copepods), as here large copepods eat smaller copepods. This clashes with the classical view of large copepods appearing in short marine food-webs, since copepods can directly feed on large primary producers, mainly diatoms. Diatoms are not represented in our unicellular model, so this effect is weakly represented.

Our model also shows a dominance in numbers by small copepods (juveniles and adults) in most cases. This was already highlighted by Turner (2004). Hopcroft, Roff, and Chavez (2001) showed that small copepods tend to dominate in most systems, and that as productivity increases large copepods appear while coexisting with small copepods. The numerical dominance of small copepods follows from the Sheldon spectrum with biomass being roughly flat with body mass (Sheldon, Prakash, and Sutcliffe Jr, 1972).

Finally, small active feeding copepods do no emerge in the system. In the model, this is due to competition with protists and predation by larger copepods. The lack of small active feeders matches with what is observed in nature. Some of the smallest active feeders are from the genus *Acartia*, where the adults tend to be larger than 1 µgC. In fact, *Acartia* tend to be mixed feeders, i.e. they can switch from active to passive feeders (Brun, Payne, and Kiørboe, 2016b). Thus, when being very small, a passive feeding strategy is favoured.

4.3.2 Feeding mode

Small passive feeders coexist with active feeders, but dominate at relatively low levels of productivity. Data compiled by Prowe et al. (2018) shows a larger fraction of passive feeding copepods (in terms of abundances) in temperate systems and high latitudes relative to low latitudes. These observations contradict our findings (assuming that high latitude systems are more productive than low latitude systems). Prowe et al. (2018) attributed this observation to the relation between feeding mode and the motility of prey (Kiørboe, 2011), which we did not include in the model. However, Djeghri et al. (2018) argued that copepods are highly prey-unselective and that motility could not be the only explanation for this pattern. Predation can be another explanation, where predators could be more abundant in productive systems, favouring the passive-feeding strategy. On the other hand, in our seasonal scenario, passive and active feeders coexist over the whole year. This indicates that seasonality could also promote this coexistence. This agrees with *Oithona sp*. (a passive feeder) being present in most marine systems (Gallienne and Robins, 2001) together with active feeding copepods (e.g. Djeghri et al., 2018).

4.4 Seasonal environment

The need of copepods to grow and develop results in a delay between the protists spring bloom and the peak in biomass of copepods in our seasonal scenario. This loop-hole is one of the reasons that phytoplankton blooms can form, where predators are not able to keep-up with the prey's growth rate, allowing for biomass accumulation of the prey (Kiørboe, 1993; Behrenfeld and Boss, 2018). The delay between the peaks in copepods and protists has been observed in several systems (Dagg, 1995; Parsons, 1988; Parsons and Lalli, 1988). This coupling between prey and predators has important implications for carbon export, since a highly coupled system results in most of the energy staying in the upper-ocean food-web, while uncoupled systems allow for a dominance of the detrital pathways, contributing to benthic production and carbon sequestration (Parsons, 1988). The delay and the decoupling would not have been observed if the ontogeny of copepods was not incorporated in the model.

4.5 Fecal pellets export

Fecal pellets export increases with the biomass of copepods in the mixed layer, but is affected by several other factors. In our steady environment scenario, trophic transfer from the mixed layer to the deep ocean is enhanced when large copepods are present. This is due to their production of fast-sinking pellets, in agreement with the results found in Stamieszkin et al. (2015). In contrast, in the seasonal scenario, transfer efficiency of fecal pellets mainly relates to the dynamics of the mixed layer. The strong relation to the integrated biomass within the mixed layer might be due to the model assumption that copepod concentration is homogeneous in the mixed layer. This does not happen in nature as most copepods spread over deeper layers (e.g. Irigoien and Harris, 2006) and swim to the surface at night to feed, probably resulting in lower integrated biomass over the mixed layer.

The attenuation of the fecal pellets flux by copepod consumption agrees with the results found in the field by Riser et al. (2007) and Riser et al. (2008), where a large fraction of the pellets produced were respired in the upper water column by copepods. Thus, the larger the copepod biomass in the water column, the larger the export flux, but the higher the consumption of fecal pellets as well.

4.6 Trophic interactions

Our model shows a high number of trophic interactions, and due to the large overlap in size, practically any kind of prey (protists, nauplii or adult copepods) can be predated on by copepods. This broad prey range on copepods has also been observed in empirical and experimental studies (Djeghri et al., 2018). Predation by copepods has a strong effect on the system, especially on small copepods, both juveniles and adults. In general, small passives dominate relative to small active feeders. By being passive feeders, they can reduce their predation mortality, while the small active feeders do not manage to reach adulthood in summer as predation on the juvenile stages is too strong. Predation by large copepods is common in nature, and predation on the juvenile stages is also well known (Uye and Liang, 1998; Ohman and Hirche, 2001).

Intraguild predation (IGP) is ubiquitous in the food-webs produced by our model. IGP is the process of "eating your own competitor" (Polis, Myers, and Holt, 1989). It often occurs when individuals undergo trophic niche shifts where a juvenile competes for prey with another consumer and where the adult predates on that consumer. The general result of IGP is that the consumer outcompetes the predator at low levels of productivity . At medium productivities the predator and consumer coexist, while the predator dominates at high productivities (Mylius et al., 2001; Hartvig and Andersen, 2013). This result is hard to track in the model since IGP occurs at several levels simultaneously, e.g., between protists and small copepods, and between small copepods and larger copepods.

Finally, competition between protists and small copepods is an interaction that is rarely considered in the literature. Still, Gismervik and Andersen (1997) found IGP to occur between a protist and a small copepod, as observed in our model. Looking at predator-prey mass ratios of zooplankton (Hansen, Bjornsen, and Hansen, 1994; Kiørboe, 2016) and the overlapping sizes of small copepods and large unicellular protists, we suggest that competition between protists and small/juveniles copepods is likely to occur in natural systems.

4.7 Model limitations

The model only represents two axes of multicellular diversity: adult size and feeding mode. This means that important factors are not represented: difference between development and somatic growth, sac/broadcast spawning, reserves, and vertical migrations. Ignoring these traits has implications for the model's ability to represent important ecosystem functions. On the other hand,

adding them increases model complexity.

The main limitation in the seasonal system is the lack of overwintering and resting eggs strategies. The production of reserves allows copepods to overwinter, often performing ontogenetic migrations, to overcome the winter months (Varpe, 2012). Copepods that perform ontogenetic vertical migrations are of high ecological importance in high latitude systems (e.g. Pershing and Stamieszkin, 2019). Reserves are also important for deep-water copepods to survive for long periods without food (Teuber et al., 2018). Another strategy, mainly performed by coastal copepods, is the production of resting eggs that survive the winter (Holm et al., 2018). The importance of reserves and vertical strategies has been demonstrated in optimisation models (Varpe, 2012; Sainmont et al., 2014), however, implementation in full population dynamic models is challenging as it introduces an extra state variable (but see de Roos and Persson, 2001).

An important difference between copepods is between broadcast and sac spawners (Kiørboe and Sabatini, 1994). Broadcast spawners release their eggs directly in the water column, which puts the eggs at risk, yet more eggs are produced and the time until hatching is faster than in sac spawning copepods. Sac spawners carry their eggs until hatching. This substantially reduces mortality. However, if the female is eaten, the whole clutch is lost. The difference between sac and broadcast spawners could be represented as another trait, and the trade-off implemented as a difference in recruitment efficiency ϵ_e and mortality of the mother.

Food-dependent growth is well represented, but the development time is known to vary with temperature (Corkett and McLaren, 1970; Berggreen, Hansen, and Kiørboe, 1988), resulting in variable adult copepod sizes of the same species. Adult size decreases up to 3% per degree increase in temperature (Horne et al., 2019). The variation in development time between birth to maturity means that the adult size is not fixed, and that somatic growth and development should be considered separately. A potential implementation could be to make the adult size temperature dependent (e.g. Maps, Pershing, and Record, 2012).

Finally, in terms of the model analysis, we have not tested for the existence of multiple stable states. Physiologically size-structured models may possess multiple stable states, either as an Allee effect (both an extinct and a non-extinct state exists; de Roos, Persson, and McCauley, 2003) or as two different states of presence (Claessen and de Roos, 2003). Capturing such states requires a complete bifurcation analysis that also tracks unstable states, such as via continuation (e.g. Kuznetsov, 2013). We have been unable to perform continuation in this system with many state variables. It is still an

open question, then, whether multiple stable states exists, and whether they are important for the overall community structure and dynamics.

5 Conclusion and perspective

The NUM (nutrients - unicellular - multicellular) modelling paradigm offers a route to resolve the importance of the role of multicellular organisms in planktonic food webs. The model reproduces macroecological patterns, coexistence of several sizes and feeding modes, and the introduction of a time-lag in the seasonal development of planktonic systems. An unexpected result is the competition between protists and small/juvenile copepods. We suggest that this interaction, together with predation, explains why the smallest adult copepods are not active feeders, favouring the passive feeding strategy within these size ranges. Finally we show that intraguild predation is ubiquitous in marine food-webs due to the increase in size over the life of multicellular organisms. Overall this model serves as a platform to study interactions within marine food-webs and generate hypotheses to be empirically validated.

We have demonstrated a framework for NUM modelling and implemented it in a simple chemostat description of the upper water column. The framework is generic and can be implemented in more realistic physical environments, such as a water column or a global circulation model. The model has been designed such that it can accommodate a variable number of size classes and populations. The advantage of the size- and trait-based formulation is a relatively small parameter set that is generic, i.e., it is valid globally and also for reduced model configurations. We envision the NUM modelling framework as a key element in developing global-scale ecosystem models that span from biogeochemistry to fish ecology.

Acknowledgements

This work was supported by the Gordon and Betty Moore Foundation through award 5479, and by the Centre for Ocean Life, a VKR Centre for Excellence funded by the Villum Foundation. F. Soudijn acknowledges support from the People Programme (Marie Curie Actions) of the European Union's Seventh Framework Programme (FP7/2007-2013) under Research Executive Agency grant agreement number 609405 (COFUNDPostdocDTU).

References

Almeda, Rodrigo, Hans van Someren Gréve, and Thomas Kiørboe (2017). "Behavior is a major determinant of predation risk in zooplankton". In: *Ecosphere* 8.2, e01668.

Andersen, Ken H (2019). *Fish Ecology, Evolution, and Exploitation: A New Theoretical Synthesis*. Vol. 93. Monographs in Population Biology. Princeton University Press.

Andersen, Ken Haste and Jan E Beyer (2006). "Asymptotic size determines species abundance in the marine size spectrum". In: *The American Naturalist* 168.1, pp. 54–61.

Andersen, Ken Haste et al. (2016). "Characteristic sizes of life in the oceans, from bacteria to whales". In:

Anderson, TR, WC Gentleman, and A Yool (2015). "EMPOWER-1.0: an Efficient Model of Planktonic ecOsystems WrittEn in R". In: *Geoscientific Model Development* 8.7, pp. 2231–2262.

Banas, N S (2011). "Adding complex trophic interactions to a size-spectral plankton model: Emergent diversity patterns and limits on predictability". In: *Ecological Modelling* 222, pp. 2663–2675.

Behrenfeld, Michael J and Emmanuel S Boss (2014). "Resurrecting the ecological underpinnings of ocean plankton blooms". In:

— (2018). "Student's tutorial on bloom hypotheses in the context of phytoplankton annual cycles". In: *Global change biology* 24.1, pp. 55–77.

Berggreen, U, B Hansen, and Thomas Kiørboe (1988). "Food size spectra, ingestion and growth of the copepodAcartia tonsa during development: Implications for determination of copepod production". In: *Marine biology* 99.3, pp. 341–352.

Bonnet, Delphine, Josefin Titelman, and Roger Harris (2004). "Calanus the cannibal". In: *Journal of Plankton Research* 26.8, pp. 937–948.

Boudreau, P R and L M Dickie (1992). "Biomass spectra of aquatic ecosystems in relation to fisheries yield." In: *Canadian Journal of Fisheries and Aquatic Science* 49.8, pp. 1528–1538.

Brun, Philipp, Mark R Payne, and Thomas Kiørboe (2016a). "Trait biogeography of marine copepods–an analysis across scales". In: *Ecology letters* 19.12, pp. 1403–1413.

Brun, Philipp Georg, Mark R Payne, and Thomas Kiørboe (2016b). "A trait database for marine copepods". In: *Earth System Science Data Discussions*, pp. 1–33.

Chakraborty, Subhendu, Lasse Tor Nielsen, and Ken H Andersen (2017). "Trophic strategies of unicellular plankton". In: *The American Naturalist* 189.4, E77–E90.

Chisholm, Laurie A and John C Roff (1990). "Size-weight relationships and biomass of tropical neritic copepods off Kingston, Jamaica". In: *Marine Biology* 106.1, pp. 71–77.

Claessen, David and Andre M de Roos (2003). "Bistability in a size-structured population model of cannibalistic fish—a continuation study". In: *Theoretical Population Biology* 64.1, pp. 49–65.

Corkett, CJ and IA McLaren (1970). "Relationships between development rate of eggs and older stages of copepods". In: *Journal of the Marine Biological Association of the United Kingdom* 50.1, pp. 161–168.

Dagg, MJ (1995). "Copepod grazing and the fate of phytoplankton in the northern Gulf of Mexico". In: *Continental Shelf Research* 15.11-12, pp. 1303–1317.

de Roos, André M and Lennart Persson (2001). "Physiologically structured models–from versatile technique to ecological theory". In: *Oikos* 94.1, pp. 51–71.

de Roos, Andre M and Lennart Persson (2013b). *Population and community ecology of ontogenetic development*. Princeton University Press, p. 448. ISBN: 978-1-4008-4561-3. DOI: 10.2307/j.ctt1r2g73.

de Roos, André M and Lennart Persson (2013a). *Population and community ecology of ontogenetic development*. Vol. 59. Princeton University Press.

de Roos, André M., Lennart Persson, and Edward McCauley (2003). "The influence of size-dependent life-history traits on the structure and dynamics of populations and communities". In: *Ecology Letters* 6.5, pp. 473–487. ISSN: 1461023X. DOI: 10.1046/j.1461-0248.2003.00458.x. URL: http://doi.wiley.com/10.1046/j.1461-0248.2003.00458.x.

de Roos, André M et al. (2008). "Simplifying a physiologically structured population model to a stage-structured biomass model". In: *Theoretical population biology* 73.1, pp. 47–62.

Djeghri, Nicolas et al. (2018). "High prey-predator size ratios and unselective feeding in copepods: A seasonal comparison of five species with contrasting feeding modes". In: *Progress in Oceanography* 165, pp. 63–74.

Ducklow, Hugh W, Deborah K Steinberg, and Ken O Buesseler (2001). "Upper ocean carbon export and the biological pump". In: *OCEANOGRAPHY-WASHINGTON DC-OCEANOGRAPHY SOCIETY-* 14.4, pp. 50–58.

Evans, Geoffrey T and John S Parslow (1985). "A model of annual plankton cycles". In: *Biological oceanography* 3.3, pp. 327–347.

Fasham, MJR, HW Ducklow, and SM McKelvie (1990). "A nitrogen-based model of plankton dynamics in the oceanic mixed layer". In: *Journal of Marine Research* 48.3, pp. 591–639.

Flynn, Kevin J and Per Juel Hansen (2013). "Cutting the canopy to defeat the "selfish gene"; conflicting selection pressures for the integration of phototrophy in mixotrophic protists". In: *Protist* 164.6, pp. 811–823.

Follows, Michael J. and Stephanie Dutkiewicz (2011). "Modeling diverse communities of marine microbes." In: *Annual review of marine science* 3, pp. 427–51. ISSN: 1941-1405. DOI: 10.1146/annurev-marine-120709-142848. URL: http://www.ncbi.nlm.nih.gov/pubmed/21329212.

Franks, P. J. S. (2002). "NPZ Models of Plankton Dynamics: Their Construction, Coupling to Physics, and Application". In: *journal of oceangraphy* 58, pp. 379–387.

Fulton, Elizabeth A (2010). "Approaches to end-to-end ecosystem models". In: *Journal of Marine Systems* 81.1-2, pp. 171–183.

Gallienne, CP and DB Robins (2001). "Is Oithona the most important copepod in the world's oceans?" In: *Journal of Plankton Research* 23.12, pp. 1421–1432.

Gentleman, Wendy (2002). "A chronology of plankton dynamics in silico: how computer models have been used to study marine ecosystems". In: *Hydrobiologia* 480.1-3, pp. 69–85.

Gismervik, Ingrid and Tom Andersen (1997). "Prey switching by Acartia clausi: experimental evidence and implications of intraguild predation assessed by a model". In: *Marine Ecology Progress Series* 157, pp. 247–259.

Hansen, Agnethe Nøhr and André W Visser (2019). "The seasonal succession of optimal diatom traits". In: *Limnology and Oceanography* 64.4, pp. 1442–1457.

Hansen, Benni, Peter Koefoed Bjornsen, and Per Juel Hansen (1994). "The size ratio between planktonic predators and their prey". In: *Limnology and oceanography* 39.2, pp. 395–403.

Hartvig, Martin, Ken H Andersen, and Jan E Beyer (2011). "Food web framework for size-structured populations". In: *Journal of theoretical Biology* 272.1, pp. 113–122.

Hartvig, Martin and Ken Haste Andersen (2013). "Coexistence of structured populations with size-based prey selection." In: *Theoretical population biology* 89, pp. 24–33. ISSN: 1096-0325. DOI: 10.1016/j.tpb.2013.07.003. URL: http://www.ncbi.nlm.nih.gov/pubmed/23927897.

Heneghan, Ryan F et al. (2016). "Zooplankton are not fish: improving zooplankton realism in size-spectrum models mediates energy transfer in food webs". In: *Frontiers in Marine Science* 3, p. 201.

Hirst, A G and T Kiørboe (2002). "Mortality of marine planktonic copepods: global rates and patterns". In: *Marine Ecology Progress Series* 230, pp. 195–209. ISSN: 01718630. DOI: 10.3354/meps230195. URL: http://www.int-res.com/abstracts/meps/v230/p195-209/.

Ho, Pei-Chi et al. (2019). "Body size, light intensity, and nutrient supply determine plankton stoichiometry in mixotrophic plankton food webs". In:

Holm, Mark Wejlemann et al. (2018). "Resting eggs in free living marine and estuarine copepods". In: *Journal of Plankton Research* 40.1, pp. 2–15.

Hopcroft, RR, JC Roff, and FP Chavez (2001). "Size paradigms in copepod communities: a re-examination". In: *Hydrobiologia* 453.1, pp. 133–141.

Horne, Curtis R et al. (2019). "Rapid shifts in the thermal sensitivity of growth but not development rate causes temperature–size response variability during ontogeny in arthropods". In: *Oikos* 128.6, pp. 823–835.

Irigoien, Xabier and Roger P Harris (2006). "Comparative population structure, abundance and vertical distribution of six copepod species in the North Atlantic: Evidence for intraguild predation?" In: *Marine Biology Research* 2.4, pp. 276–290.

Kiørboe, T and Marina Sabatini (1995). "Scaling of fecundity, growth and development in marine planktonic copepods". In: *Marine ecology progress series. Oldendorf* 120.1, pp. 285–298.

Kiørboe, Thomas (1993). "Turbulence, phytoplankton cell size, and the structure of pelagic food webs". In: *Advances in marine biology*. Vol. 29. Elsevier, pp. 1–72.

— (2011). "How zooplankton feed: mechanisms, traits and trade-offs". In: *Biological Reviews* 86.2, pp. 311–339.

— (2016). "Foraging mode and prey size spectra of suspension-feeding copepods and other zooplankton". In: *Marine Ecology Progress Series* 558, pp. 15–20.

Kiørboe, Thomas and Andrew G Hirst (2014). "Shifts in mass scaling of respiration, feeding, and growth rates across life-form transitions in marine pelagic organisms". In: *The American Naturalist* 183.4, E118–E130.

Kiørboe, Thomas and Marina Sabatini (1994). "Reproductive and life cycle strategies in egg-carrying cyclopoid and free-spawning calanoid copepods". In: *Journal of Plankton Research* 16.10, pp. 1353–1366.

Kiørboe, Thomas, André Visser, and Ken H Andersen (2018). "A trait-based approach to ocean ecology". In: *ICES Journal of Marine Science* 75.6, pp. 1849–1863.

Kuznetsov, Yuri A (2013). *Elements of applied bifurcation theory*. Vol. 112. Springer Science & Business Media.

Leles, Suzana GonÇalves et al. (2018). "Modelling mixotrophic functional diversity and implications for ecosystem function". In: *Journal of Plankton Research* 40.6, pp. 627–642.

Longhurst, Alan et al. (1995). "An estimate of global primary production in the ocean from satellite radiometer data". In: *Journal of plankton Research* 17.6, pp. 1245–1271.

Maps, Frédéric, Andrew J Pershing, and Nicholas R Record (2012). "A generalized approach for simulating growth and development in diverse marine copepod species". In: *ICES journal of marine science* 69.3, pp. 370–379.

Mauchline, John (1998). "The biology of calanoid copepods". In: *Adv. Mar. Biol.* 33, pp. 1–710.

May, Robert M (1973). "Time-delay versus stability in population models with two and three trophic levels". In: *Ecology* 54.2, pp. 315–325.

McCauley, Edward and William W Murdoch (1987). "Cyclic and stable populations: plankton as paradigm". In: *The American Naturalist* 129.1, pp. 97–121.

McGurk, Michael D (1986). "Natural mortality of marine pelagic fish eggs and larvae: role of spatial patchiness". In: *Marine Ecology Progress Series* 34, pp. 227–242. ISSN: 0171-8630. DOI: 10.3354/meps034227.

Mitra, Aditee et al. (2014). "Bridging the gap between marine biogeochemical and fisheries sciences; configuring the zooplankton link". In: *Progress in Oceanography* 129, pp. 176–199.

Mylius, Sido D et al. (2001). "Impact of intraguild predation and stage structure on simple communities along a productivity gradient". In: *The American Naturalist* 158.3, pp. 259–276.

Neuheimer, A. B. et al. (2015). "Adult and offspring size in the ocean over 17 orders of magnitude follows two life-history strategies". In: *Ecology* 96.12, pp. 3303–3311.

Ohman, MD and H-J Hirche (2001). "Density-dependent mortality in an oceanic copepod population". In: *Nature* 412.6847, p. 638.

Parsons, Timothy R (1988). "Trophodynamic phasing in theoretical, experimental aud natural pelagic ecosystems". In: *Journal of the Oceanographical Society of Japan* 44.2, pp. 94–101.

Parsons, TR and CM Lalli (1988). "Comparative oceanic ecology of the plankton communities of the subarctic Atlantic and Pacific oceans". In: *Oceanogr. Mar. Biol. Ann. Rev* 26, pp. 317–359.

Pershing, Andrew J and Karen Stamieszkin (2019). "The North Atlantic Ecosystem, from Plankton to Whales". In: *Annual review of marine science* 12.

Persson, Lennart et al. (1998). "Ontogenetic scaling of foraging rates and the dynamics of a size-structured consumer-resource model". In: *Theoretical population biology* 54.3, pp. 270–293.

Polis, Gary A, Christopher A Myers, and Robert D Holt (1989). "The ecology and evolution of intraguild predation: potential competitors that eat each other". In: *Annual review of ecology and systematics* 20.1, pp. 297–330.

Prowe, AE Friederike et al. (2018). "Biogeography of zooplankton feeding strategy". In: *Limnology and Oceanography*.

Record, NR, AJ Pershing, and F Maps (2013). "Emergent copepod communities in an adaptive trait-structured model". In: *Ecological modelling* 260, pp. 11–24.

Riser, Christian Wexels et al. (2007). "Export or retention? Copepod abundance, faecal pellet production and vertical flux in the marginal ice zone through snap shots from the northern Barents Sea". In: *Polar Biology* 30.6, pp. 719–730.

Riser, Christian Wexels et al. (2008). "Vertical flux regulation by zooplankton in the northern Barents Sea during Arctic spring". In: *Deep Sea Research Part II: Topical Studies in Oceanography* 55.20-21, pp. 2320–2329.

Sainmont, Julie et al. (2014). "Capital versus Income Breeding in a Seasonal Environment". In: *The American Naturalist* 184.4, pp. 466–476. ISSN: 0003-0147. DOI: 10.1086/677926.

Serra-Pompei, Camila et al. (2019). "Resource limitation determines temperature response of unicellular plankton communities". In: *Limnology and Oceanography*.

Sheldon, RW, A Prakash, and WHr Sutcliffe Jr (1972). "THE SIZE DISTRIBUTION OF PARTICLES IN THE OCEAN 1". In: *Limnology and oceanography* 17.3, pp. 327–340.

Small, LF, SW Fowler, and MY Ünlü (1979). "Sinking rates of natural copepod fecal pellets". In: *Marine Biology* 51.3, pp. 233–241.

Sprules, W.G. and L.E. Barth (2015). "Surfing the biomass size spectrum: some remarks on history, theory, and application". In: *Canadian Journal of Fisheries and Aquatic Sciences* 73.4, pp. 477–495.

Stamieszkin, Karen et al. (2015). "Size as the master trait in modeled copepod fecal pellet carbon flux". In: *Limnology and Oceanography* 60.6, pp. 2090–2107.

Steinberg, Deborah K and Michael R Landry (2017). "Zooplankton and the ocean carbon cycle". In: *Annual Review of Marine Science* 9, pp. 413–444.

Teuber, Lena et al. (2018). "Who is who in the tropical Atlantic? Functional traits, ecophysiological adaptations and life strategies in tropical calanoid copepods". In: *Progress in oceanography*.

Tilman, David (1982). *Resource competition and community structure*. Princeton university press.

Turner, Jefferson T (2004). "The importance of small planktonic copepods and their roles in pelagic marine food webs". In: *Zoological studies* 43.2, pp. 255–266.

Ursin, Erik (1973). *On the prey size preferences of cod and dab*. Danmarks Fiskeri-og Havundersøgelser.

Uye, Shin-ichi and Dong Liang (1998). "Copepods attain high abundance, biomass and production in the absence of large predators but suffer cannibalistic loss". In: *Journal of Marine Systems* 15.1-4, pp. 495–501.

Varpe, Øystein (2012). "Fitness and phenology: annual routines and zooplankton adaptations to seasonal cycles". In: *Journal of Plankton Research* 34.4, pp. 267–276.

Ward, Ben A. and Michael J. Follows (2016). "Marine mixotrophy increases trophic transfer efficiency, mean organism size, and vertical carbon flux". In: *Proceedings of the National Academy of Sciences* 14, p. 201517118. ISSN: 0027-8424. DOI: 10.1073/pnas.1517118113. URL: http://www.pnas.org/lookup/doi/10.1073/pnas.1517118113.

Weitz, Joshua S et al. (2015). "A multitrophic model to quantify the effects of marine viruses on microbial food webs and ecosystem processes". In: *The ISME journal* 9.6, p. 1352.

Werner, Earl E and James F Gilliam (1984). "The ontogenetic niche and species interactions in size-structured populations". In: *Annual review of ecology and systematics* 15.1, pp. 393–425.

A Minimum food requirements, E*

We can obtain the E^* of the copepods by isolating E from (4) and (1):

$$E^* = \frac{h f_{\mathrm{fc}}}{v(1-f_{\mathrm{fc}})} m^{n-q}. \tag{A.1}$$

Since the exponents of maximum consumption rate and clearance rate are identical $n = q$, E^* becomes independent of body mass and corresponds to 27μgC L^{-1} for active feeders and 16μgC L^{-1} for passive feeders.

To calculate E^* for protists we first assume that they are completely heterotrophs, so we simply assume that $\nu_u(m) = \eta_E(m) - \eta_R(m)$. The E^* for protists becomes:

$$E^* = \frac{\psi_F(m)}{\alpha_F(m)\psi_F(m)/\eta_R(m) - \alpha_F(m)}. \tag{A.2}$$

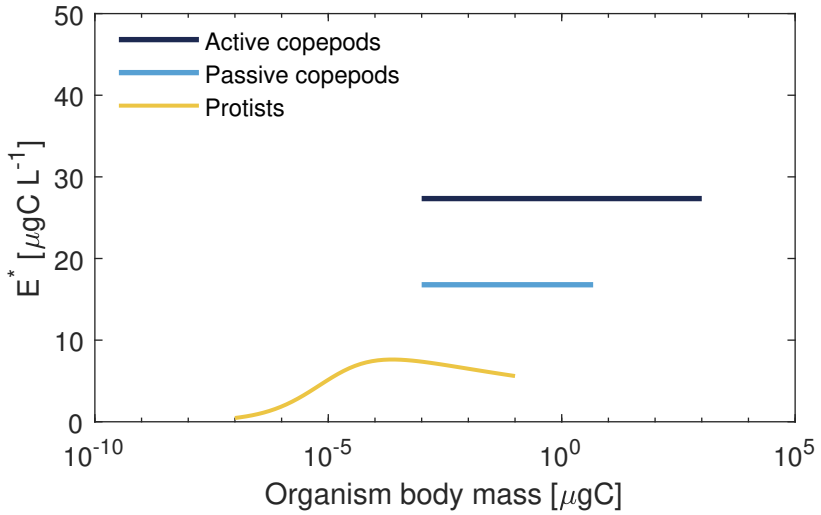

Fig. A.1. The food concentration, E^* where growth is zero for protists (yellow), and active and passive copepods (dark/light blue). Since we are interested in the competition for prey here E^* of protists is calculated in the absence of light and nutrients, i.e., considered as pure heterotrophs. See appendix A for derivation of E^*.

B Parameter values

There are 3 sets of parameters: for the copepods (Table 1 and Fig. 2), for the protists, and for the fecal pellets. Most parameters are in the form of allometric scalings obtained from literature sources or the data analyses in Fig. 2. Metabolic theory predicts that most metabolic rates scale with body mass with a 3/4 exponent, or -1/4 if rates are considered carbon-specific, i.e. per unit of carbon mass. The rates scale with a power law of the form $R = am^b$. So one of the major assumptions in this model is that all rates (except some rates for protists, justified in the following section) scale with this metabolic exponent. Exponents that differ in value introduce additional complications in the model. For example, if the exponent of metabolism is higher than the exponent of maximum consumption it introduces an absolute upper size of organisms in the system (Andersen et al., 2008). To avoid such complications arising as artifacts arising from fitting on poor data we simply fixed the exponents to be identical. In practice we did least square fits with a fixed exponent of -1/4.

B.1 Copepod parameters

B.1.1 Assimilation efficiency

Assimilation efficiency varies broadly between species and feeding conditions. We assumed a rough estimate of 2/3, which falls within observed ranges (Kiørboe, Møhlenberg, and Hamburger, 1985). But a sensitivity analysis has been performed in section D.

B.1.2 Respiration rates

Measured respiration rates are the total respiration of organisms, that is, basal metabolism and costs associated with activity such as specific dynamic action or energy used to swim. Data was obtained from Kiørboe and Hirst (2014), who corrected the data to a reference temperature of 15°C. Note that in the paper there is an error in the units for respiration in Table 1: units of respiration rate are in $mLO_2\ mgC^{-1}\ L^{-1}$ but should be in $\mu LO_2\ mgC^{-1}\ L^{-1}$. To convert to units of d^{-1} we used:

- Oxycaloric coefficient = 0.0136 KJ mgO_2^{-1} (Elliott and Davison, 1975).
- Molar weight of O_2=31.998 10^3 mg/mol.
- Molar volume of O_2 at STP = 22.4 L/mol.

- Energy content for copepods is approx 26 J mg^{-1} (Ikeda, Yamaguchi, and Matsuishi, 2006).
- 1gDW = 0.48 gC (Chisholm and Roff, 1990).

The oxycaloric coefficient then becomes:

$$OC_c = \frac{0.0136\text{KJ}}{\text{mgO}_2}\frac{31.998\ 10^3\text{mgO}_2}{\text{molO}_2}\frac{\text{molO}_2}{22.391\text{LO}_2}\frac{\text{gDW}}{26\text{KJ}}\frac{0.48\text{gC}}{\text{gDW}} = 0.36\ \text{gC}\ \text{LO}_2^{-1}. \tag{B.1}$$

B.1.3 Maximum ingestion rate

Maximum ingestion rates were derived from data of Kiørboe and Hirst (2014). There are few data points of maximum ingestion rates for ambush feeders, and the data lead to a critical feeding level (f_c) of ambush feeders that is larger than the one of active feeders. We are uncertain that this is true. Considering the (bad) fit of the data and possible artifacts in the model, we prefer to derive the maximum ingestion rate of ambush feeders assuming that they have the same critical feeding level as active feeders. Thus, assuming that assimilation efficiency is the same for both copepods, we get a coefficient for maximum ingestion rate for passive copepods of: $h = r/(\epsilon f_{\text{fc}}) = 0.048/(0.67 \times 0.18) = 0.40\ \mu\text{gC}^{1/4}\ \text{d}^{-1}$.

B.1.4 Clearance rates

Clearance rate data were obtained from Kiørboe and Hirst (2014) (Fig. 2b).

B.1.5 Reproduction and recruitment efficiencies

Reproduction efficiency takes into account the ratio of males and females and the survival of eggs until hatching. To calculate the egg survival we use estimated egg mortalities and hatching times from Kiørboe and Sabatini (1994). We obtain values of 0.37 and 0.74 for broadcast and sac spawners respectively. Since we do not distinguish between broadcast and sac-spawners in our model, we simply do the average of the two efficiencies, which gives a value of 0.5 for both feeding modes. Finally, assuming a 1:1 male to female ratio, the total reproduction efficiency becomes $\epsilon_r = 0.25$.

B.1.6 Adult-offspring mass ratio

Copepod have offspring that are proportional to the adult size. The adult:egg mass ratio varies from 100 to 1000 and differs between broadcast and sac-spawners (Kiørboe and Sabatini, 1995; Neuheimer

et al., 2015). For simplicity in the model we assume a ratio of $z_{\text{a:o}} = 100$ between the adult and our first nauplii stage.

B.1.7 Predator:prey mass ratio

Predator-prey mass ratios were taken from Kiørboe (2016). There is a wide range of preferred predator-prey mass ratios for active feeders, so we take $\beta = 10\,000$ since it is the preferred range for this feeding mode (we do a sensitivity analysis fro this parameter in appendix D). Following the same reasoning we take $\beta = 100$ for passive feeders.

The size width (σ) of the preference is rather unknown but Kiørboe (2016) found that passive feeders have a narrower preference function. We use values of 1.5 and 1 for actives and passives respectively, that allows for a wide preference function but still falling within realistic values (Hansen, Bjornsen, and Hansen, 1994).

B.1.8 Mortalities

The constant for the higher trophic level mortalities were adjusted such that total mortality – including the potential mortality by predation – with an exponent of -1/4 were similar to the analytical solutions derived in appendix F.

B.1.9 Function p_{htl} for predation by higher trophic levels.

We impose the mortality by higher trophic levels only on the copepods that are not eaten by anyone in the model (Fig. B.1). The size where this shift occurs is $m_{\text{shift}} = m_{\text{max}}/\beta$, where m_{max} is the size of the largest copepod in the model, i.e. 1000 µgC. The function is equivalent to the predator-prey preference function ϕ if the body-mass is below m_{shift} and 1 otherwise:

$$p_{\text{htl}} = \phi(m_{\text{shift}}, m_{\text{max}}), \qquad \text{if } m \leq m_{\text{shift}} \tag{B.2}$$

$$p_{\text{htl}} = 1, \qquad \text{if } m > m_{\text{shift}}. \tag{B.3}$$

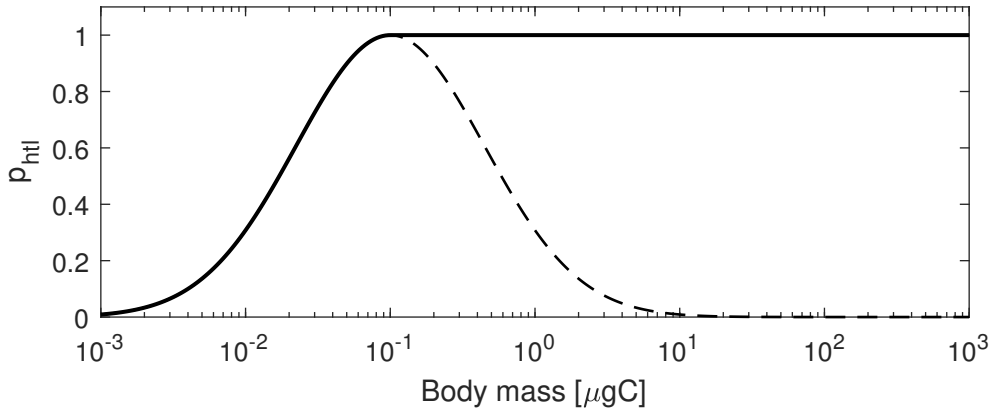

Fig. B.1. The function p_{htl} (solid). The dashed line shows $\phi(m_{\text{shift}}, m_{\text{max}})$.

B.2 Parameters Protists

B.2.1 Predator-prey mass ratio

Parameters for the preference function of prey for protists are $\beta = 500$ falling within the ranges found by Hansen, Bjornsen, and Hansen (1994) and $\sigma = 1$.

B.2.2 Affinity for nitrogen

We derived the affinity for nitrogen from Andersen et al. (2016) (appendix) where $\alpha_N = 0.0025L^1$, being L the cell diameter in cm and A_N in L d^{-1}. Converting length to mass (µgC) and making it carbon-specific we get:

$$A_N = 2.5\ 10^{-3} l^1 = 2.5\ 10^{-3} \left(\frac{1}{0.3\ 10^6}\right)^{1/3} m^{1/3} = 3.75\ 10^{-5} m^{1/3} \tag{B.4}$$

and specific nutrient affinity (L µgC^{-1} d^{-1}) is then:

$$A_N = 3.75\ 10^{-5} m^{1/3-1} = 3.75\ 10^{-5} m^{-2/3} \tag{B.5}$$

B.2.3 Affinity for Food (clearance rate)

Affinity for food (i.e. clearance rate) was fitted from the data in Kiørboe and Hirst (2014) (fig. B.2) with least squares and forced slope of -1/4. Thus, affinity for food is ((µgC L^{-1})$^{-1}$ d^{-1}):

$$\alpha_E = 0.0024 m^{-1/4}. \tag{B.6}$$

The data is sparse and there is no clear fit. In the original paper Kiørboe and Hirst (2014) one can see clear differences between flagellates and cilliates. Cilliates have a much higher clearance rate than flagellates. The data from flagellates is also sparse and does not show a clear pattern. One could think that what kind of heterotrophic protists dominates might define the clearance rate experienced. We did not want to go into more details on the protists, we thus pooled all the data together.

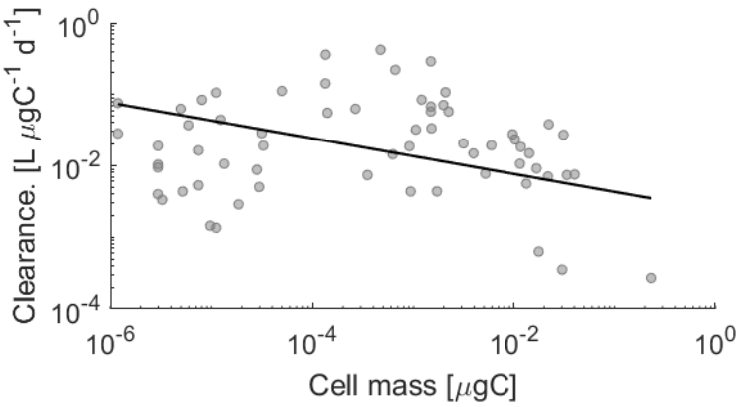

Fig. B.2. Clearance rate of protists. Dots are data from Kiørboe and Hirst (2014). Line is least square fit with forced -1/4 slope.

B.2.4 Affinity for light

Affinity for light α_L ((µE m^{-2} s^{-1})$^{-1}$ d^{-1}) was fitted from data from Edwards, Klausmeier, and Litchman (2015) and is:

$$\alpha_L = \frac{A_L m^{2/3}(1 - \exp[-c_L m^{1/3}])}{m} \tag{B.7}$$

where $c_L = 21$ and $A_L = 0.000914$.

B.2.5 Maximum Uptake rates

Maximum uptake rate for nitrogen was taken from Marañón et al. (2013), and is: $V_N = 10^{-3}V^{0.97}$ in pgN cell^{-1} h^{-1} where V is the cell volume. We used the conversion from Menden-Deuer and Lessard (2000) to convert from volume to carbon mass, and the $Q_{C:N}$ (table 1) to convert the units of nitrogen to carbon. We then get (in d^{-1}):

$$\psi_N(m) = 2.3757 m^{0.1844}. \tag{B.8}$$

Maximum photosynthetic rate was also taken from Marañón et al. (2013). Here they find a unimodal function, where they provide two fits: one for the small cells for which the exponent is positive and for the larger cells for which the exponent is negative. We thus combine both and use the minimum of both curves. After conversions we get(in d^{-1}):

$$\psi_L(m) = \min[156m^{0.37},\ 0.2792m^{-0.2442}] \tag{B.9}$$

Maximum ingestion rate was taken from Kiørboe and Hirst (2014) and is (after conversions)(in d^{-1}):

$$\psi_E = 0.1514m^{-0.33} \tag{B.10}$$

B.2.6 Respiration rate

Respiration rate is assumed to be a fraction of a maximum growth rate. The maximum growth rate $g_{\max}(m)$ of protists was taken from Ward et al. (2017) which was based on the data from Marañón et al. (2013). To convert from volume to carbon mass we used the relationship from Menden-Deuer and Lessard, 2000 (eq. B.15). Thus respiration rate in the model is $\eta_R = 0.2g_{\max}(m)$.

B.2.7 Background mortality

Similar to the respiration rate, the coefficient for the background mortality for protists (i.e. viral lysis) is a fraction of the maximum growth rate from Ward et al. (2017) and is thus: $\mu_{u,b0}(m) = 0.03_{max}/m^{-1/4}$.

B.3 Parameters fecal pellets

The volume of fecal pellets (μm^{-3}) is proportional to the body-mass (µgC) of the copepod producing it (Mauchline, 1998):

$$V_{fp} = 3.5 \times 10^4 m^{0.938}. \tag{B.11}$$

the sinking rate (m d^{-1}) was taken from Small, Fowler, and Ünlü (1979):

$$v_s = 10^{-1.214} V_{fp}^{0.513}. \tag{B.12}$$

For the purpose of copepods eating fecal pellets we need to obtain the carbon mass of each fecal pellet. The predation function of copepods considers particles in terms of their carbon mass. However, due to the high density of fecal pellets, the carbon mass is high. It would then appear that the partciles are 'larger' than they actually are. Hence, we simply obtain the carbon mass of the fecal pellets from the volume of the pellet, assuming the same conversion factor from volume to carbon mass as for phytoplankton from Menden-Deuer and Lessard (2000) (eq. B.15). Ideally, to fix this problem, the predation function should be a function of volume or length rather than carbon mass.

B.3.1 Fecal pellet flux to 1000 m

The flux of fecal pellets leaving the mixed layer (m^{-2} d^{-1}) is:

$$J_{FFP,mld} = \frac{v_s(m_l)}{z} F_l. \tag{B.13}$$

The flux of fecal pellets reaching 1000 m assuming steady state becomes:

$$J_{FFP,1000} = J_{FFP,mld} \exp[-r(z_{1000} - zmld)/v_s] \tag{B.14}$$

B.4 Conversion factors

To convert phytoplankton volume (μm^{-3}) to carbon mass (µgC $cell^{-1}$) we used the relationship from Menden-Deuer and Lessard (2000):

$$m = 10^{-0.665} V^{0.939} 10^{-6} \tag{B.15}$$

For copepods, to convert from prosome length to body mass we used the conversion factors from Chisholm and Roff (1990) of combined calanoid copepods.

$$\ln W = 2.74 \ln L - 16.41 \tag{B.16}$$

Where W is body mass in µgAFDW and L prosome length in µm. Converting body-mass to µgC using 1gDW=0.48gC also from Chisholm and Roff (1990) and a ratio of 0.73 between AFDW:DW we get:

$$m = 0.73 \times 0.48 \exp[-16.41] L.^{2.74}; \tag{B.17}$$

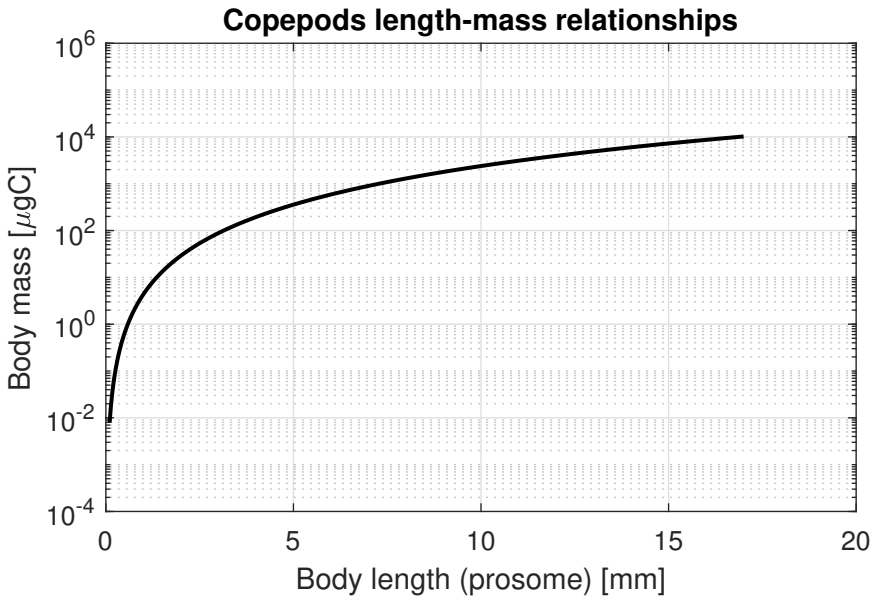

Fig. B.3. Prosome length to body-mass of relationship for copepods found in Chisholm and Roff (1990). Conversion factor from ash free dry weight (AFDW) to gC was assuming a 0.73 ratio of AFDW:DW and a conversion of 1 gDW=0.48 gC (Chisholm and Roff, 1990). Note that prosome length is in mm and not µ as in Chisholm and Roff, 1990.

1034 Where L is prosome length in µm and m body carbon mass in µgC.

C Physical forcing in the seasonal environment

We use the same approach as in Evans and Parslow (1985) and Fasham, Ducklow, and McKelvie (1990). State variables are differently affected by the rate of change of the mixed layer ($z' = \mathrm{d}z/\mathrm{d}t$). Nutrients enter the mixed layer when there is entrainment ($z' > 0$) and by a background diffusive term (ω). Hence, the input-rate ρ of nitrogen averaged over the mixed layer becomes:

$$\rho(t) = \frac{\omega + \max(0, z'(t))}{z(t)}. \tag{C.1}$$

Protists and detritus are similarly affected by the mixed layer. When the mixed layer deepens ($z'(t) > 0$) particles are diluted within the mixed layer (per unit volume, but maintained per unit area), whereas when the mixed layer shallows ($z'(t) < 0$) particles are lost from the mixed layer (assuming cells do not swim). Hence, in the protists and fecal pellets equations, eqs. 21 and 30, we add $\rho(t)P_j$ and $\rho(t)F_k$ respectively. Copepods are assumed to be able to regulate their position in the water column, and therefore are diluted when the mixed layer increases, but are up-concentrated when it decreases, hence we add the term $-z'(t)/z(t)C_{i,s}$ to equations 9, 10 and 11.

Light is the average irradiance within the mixed layer and is a function of latitude, cloudiness, mixed layer depth, and concentration of protists. The attenuation coefficient of light in the water is:

$$k_{\mathrm{tot}} = k_{\mathrm{w}} + k_{\mathrm{chl}} \sum_{j=1}^{n_{\mathrm{u}}} P_j, \tag{C.2}$$

where k_{w} is the attenuation coefficient of water (m^{-1}) and k_{chl} the attenuation of light by protists ($(\mu\mathrm{gC\ L}^{-1})^{-1}\ \mathrm{m}^{-1}$). We assume that the light experienced by protists in the depth-averaged irradiance within the mixed layer:

$$L(I_0, z) = \delta_{\mathrm{PAR}}\delta_{\mathrm{clouds}} \frac{I_0(t,l)}{k_{\mathrm{tot}} z(t)} (1 - \exp[-k_{\mathrm{tot}} z(t)]), \tag{C.3}$$

where $I_0(t,l)$ is the daily averaged irradiance at the top of the atmosphere (as a function of latitude and time), δ_{PAR} is the ratio of PAR to total irradiance, and δ_{clouds} is a measure of the attenuation by clouds and is $\delta_{\mathrm{clouds}} = 1 - c_{\mathrm{okt}}$ where c_{okt} is a measure of cloudiness. All parameter values of environmental forcing for both scenarios can be found in table 2.

Symbol	Name	Units	Steady environment	Seasonal environment
L	Irradiance	μE s^{-1} m^{-2}	30	Eq.C.3
N_0	Nitrogen concentration deep layer	µgN L^{-1}	140	140
T	Temperature	°C	15	fig.C.1
ρ	Input rate of particles in the mixed layer	d^{-1}	varies	Eq.C.1
z	depth horizon	m	10	z_{mld} fig.C.1
δ_{PAR}	PAR:total irradiance	-		0.4
c_{okt}	Cloudiness	Oktas	-	5
k_w	Attenuation coefficient of water	m^{-1}	-	0.04
r	Remineralisation rate	d^{-1}	-	0.05
δ	Fraction of dead matter going to N	-	-	0.05
ρ_{seed}	Seeding rate	d^{-1}	-	$hm^n \times 10^{-3}$
$_{seed}$	Seeding biomass	µgC L^{-1}	-	$1\Delta 10^{-3}/m$
Δ	width of each size group	µgC	-	

Table 2. Parameters environmental forcing

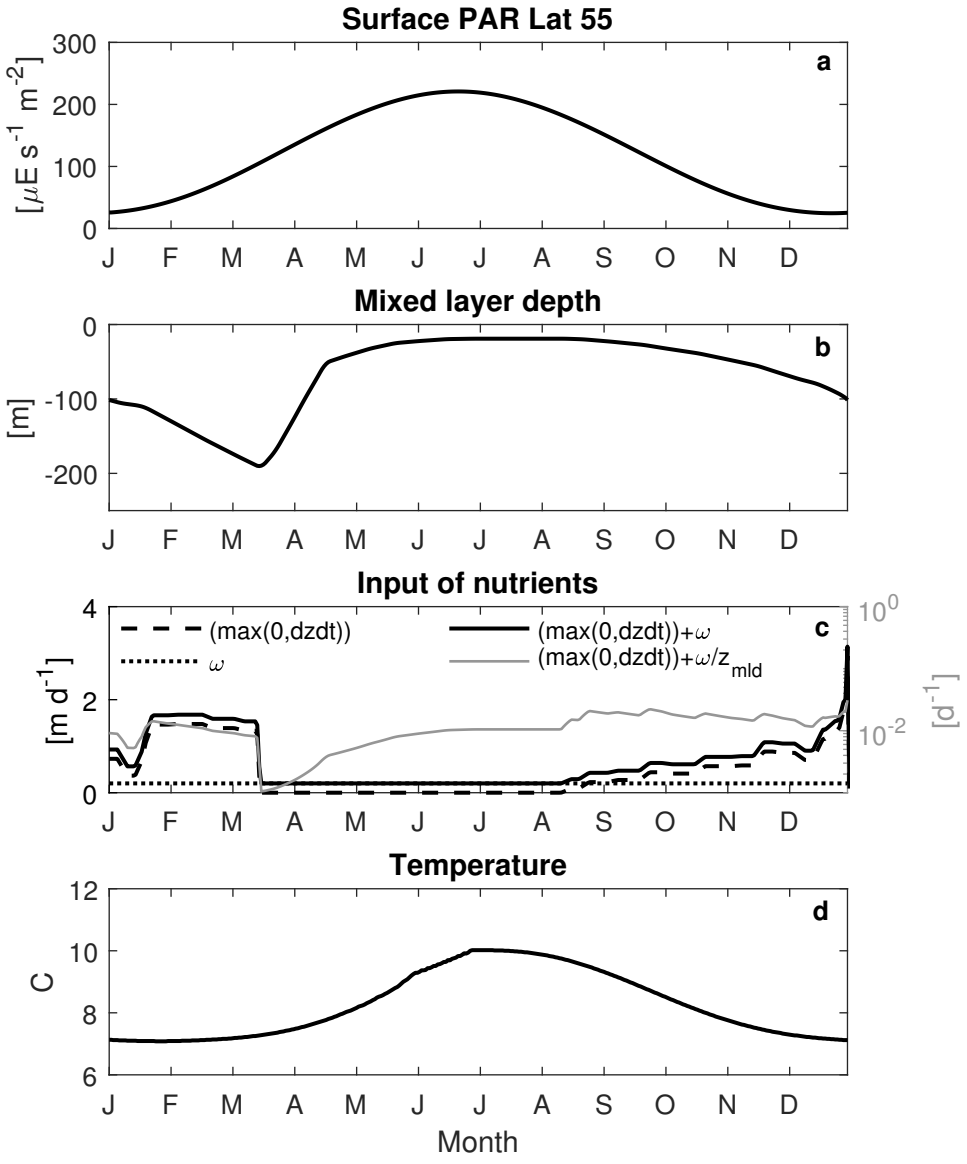

Fig. C.1. Environmental forcing for the seasonal scenario. (a) daily surface irradiance, converted to photosynthetically active radiation (PAR) by assuming a ratio of 0.4. (b) is the mixed layer depth in m. (c) is the ρ function for the seasonal scenario and each line represent one part of this function as noted in the legend. Here $N_0 = 140 \mu g N L^{-1}$. (d) is average temperature in the mixed layer characteristic from an open ocean system.

D Sensitivity analysis

We performed a sensitivity analysis for some selected parameters: number of stages in each copepod population (fig. D.1 and D.2), predator-prey mass ratio for active feeders β (fig. D.3), width of the predator-prey mass ratio σ for active feeders (fig. D.4), and the assimilation efficiency ϵ (fig. D.5).

D.0.1 Number of stages in each copepod population

We performed a sensitivity analysis for the number of stages in the copepod model. We ran the model with 14 size groups of protists, one population of active copepods, and one population of passive copepods and 6 size classes of fecal pellets. We ran the model for 20000 days in a steady environment with $\rho = 0.05$ d^{-1}, $N_0 = 140$ µgN L^{-1}, $T = 15$ °C and light being 100µE s^{-1} m^{-2}.

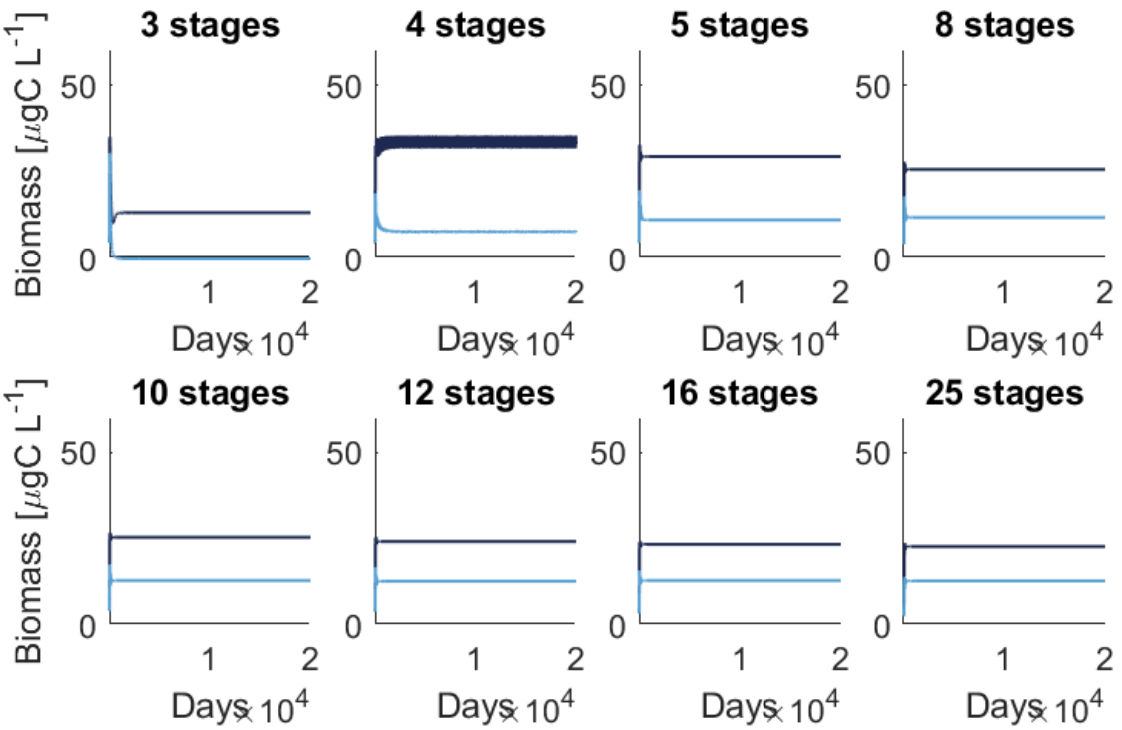

Fig. D.1. Runs of the model for different number of stages within each copepod populations. Lines show total biomass of the active copepod population (dark blue) and passive population (light blue). What looks like a thick line in pannel 2 are oscillations.

D.0.2 Parameters sweep

Different predator-prey mass ratios (β) for active feeders result in different copepod sizes coexisting (Appendix D, fig. D.3). At high productivity levels ($\rho = 0.05$ d^{-1}), small ratios ($\beta \sim 10$) result in small and intermediate copepods dominating, whereas large ratios ($\beta > 10^4$) results in mainly large copepods dominating the system. Intermediate ranges of β ($100 < \beta < 10^4$) result in the coexistence of all sizes of active feeders.

Variations in the width (σ) of the prey preference function of active feeders (fig. D.4) show that $\sigma < 1$ removes active feeders from the system, leaving only passive feeders. On the other hand $\sigma > 1.8$ removes passive feeders, and further increases in this parameters do not seem to change the dynamics of active feeders. Intermediate ranges result in the coexistence of both feeding modes.

Variations in the assimilation efficiency for all copepods mainly affects the fecal pellets flux (fig. D.5). Intermediate assimilation efficiencies ($\epsilon = 0.5$) result in the higher carbon flux, as copepods can grow but most of the food is excreted in the form of fecal pellets. ($\epsilon = 0.3$) kills most copepods, whereas large efficiencies results in higher copepods coexistence but reduced

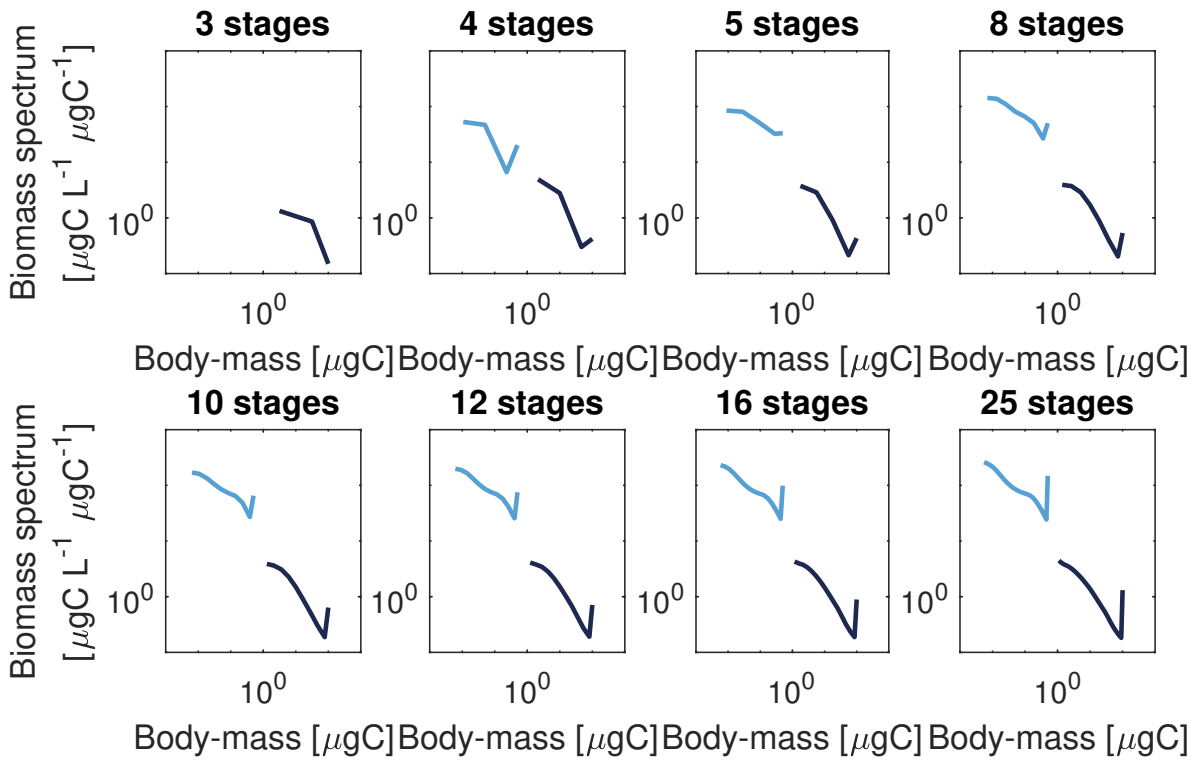

Fig. D.2. Biomass spectrum of each population for different number of stages within the copepod populations of active feeders (dark blue) and passive feeders (light blue).

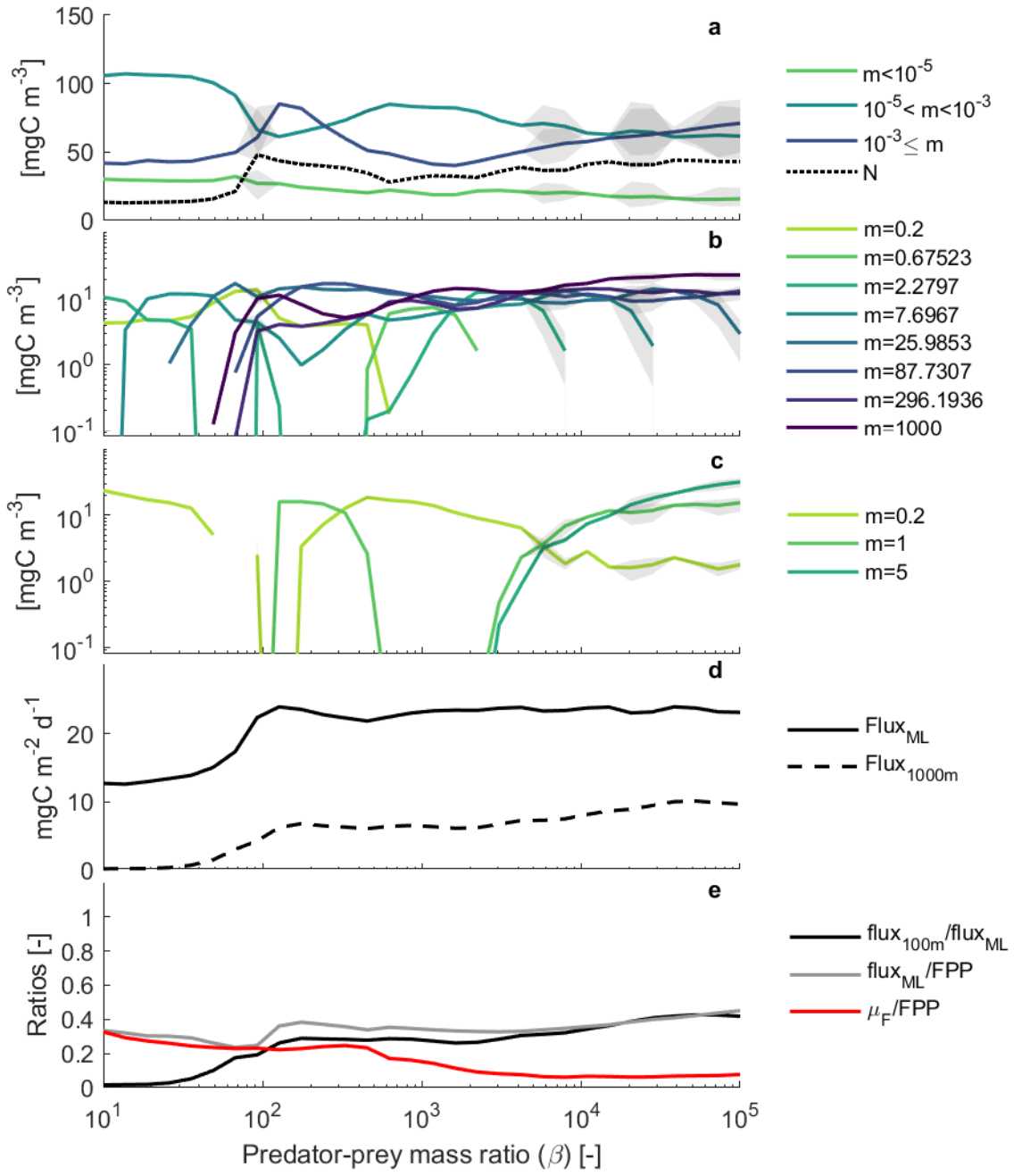

Fig. D.3. Parameter sweep for the predator-prey mass ratio (β) of active feeders only. (**a**) Protists grouped by size-ranges as stated in the legend. (**b**) active copepods and (**c**) passive copepods. Shaded areas around the lines show maximum and minimum biomass values when the system oscillates. (**d**) Fecal pellets export from the mixed layer ($Flux_{ML}$) and at 1000m ($Flux_{1000}$). (**e**) Transfer efficiency: fraction of pellets exported out of the mixed layer that reach 1000 m (black), fraction of fecal pellets produced that are exported out of the mixed layer (grey), and fraction of pellets produced that are consumed by copepods (red).

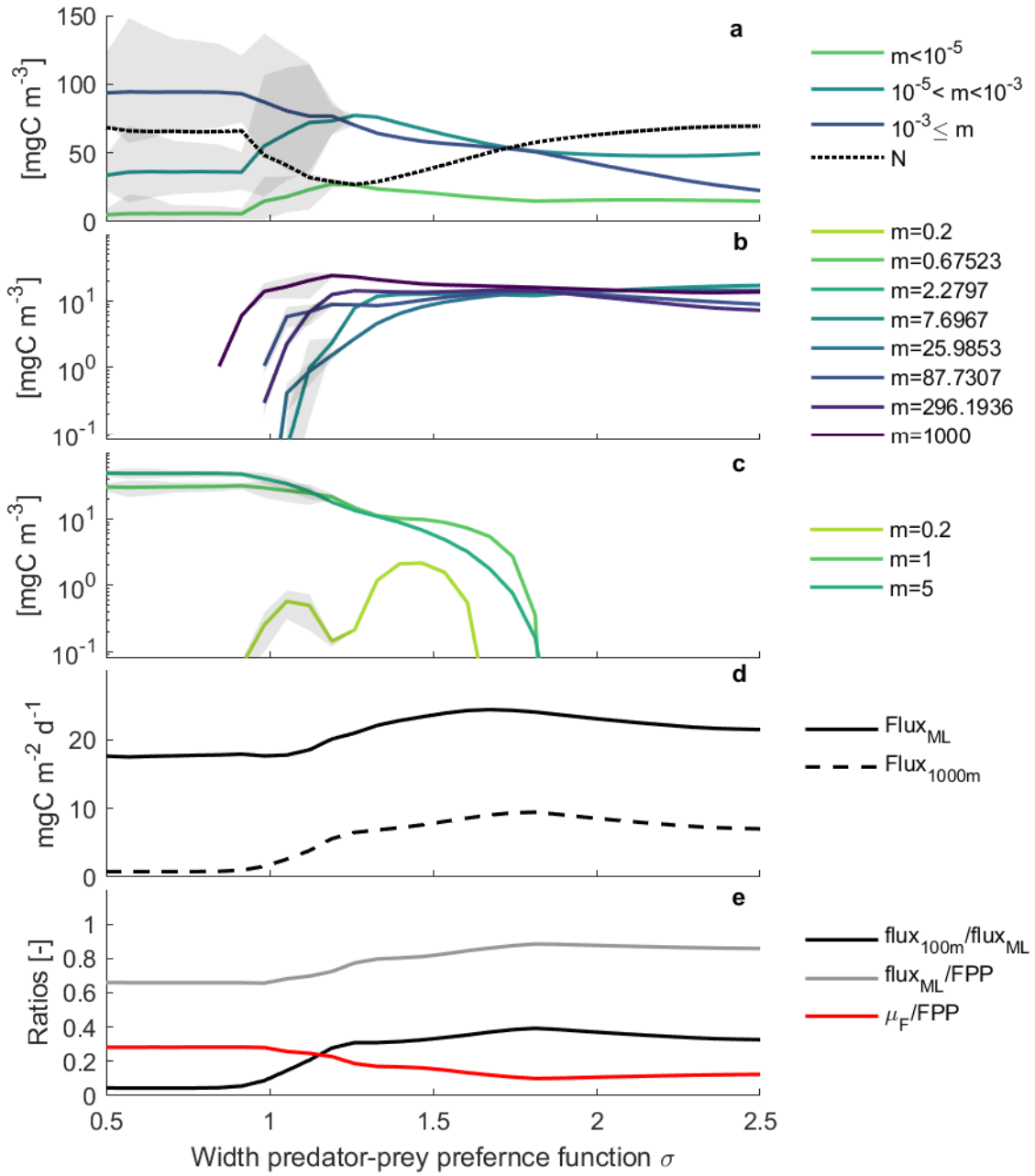

Fig. D.4. Parameter sweep for the width (σ) of the preference function for prey of active feeders. (**a**) Protists grouped by size-ranges as stated in the legend. (**b**) active copepods and (**c**) passive copepods. Shaded areas around the lines show maximum and minimum biomass values when the system oscillates. (**d**) Fecal pellets export from the mixed layer ($Flux_{ML}$) and at 1000m ($Flux_{1000}$). (**e**) Transfer efficiency: fraction of pellets exported out of the mixed layer that reach 1000 m (black), fraction of fecal pellets produced that are exported out of the mixed layer (grey), and fraction of pellets produced that are consumed by copepods (red).

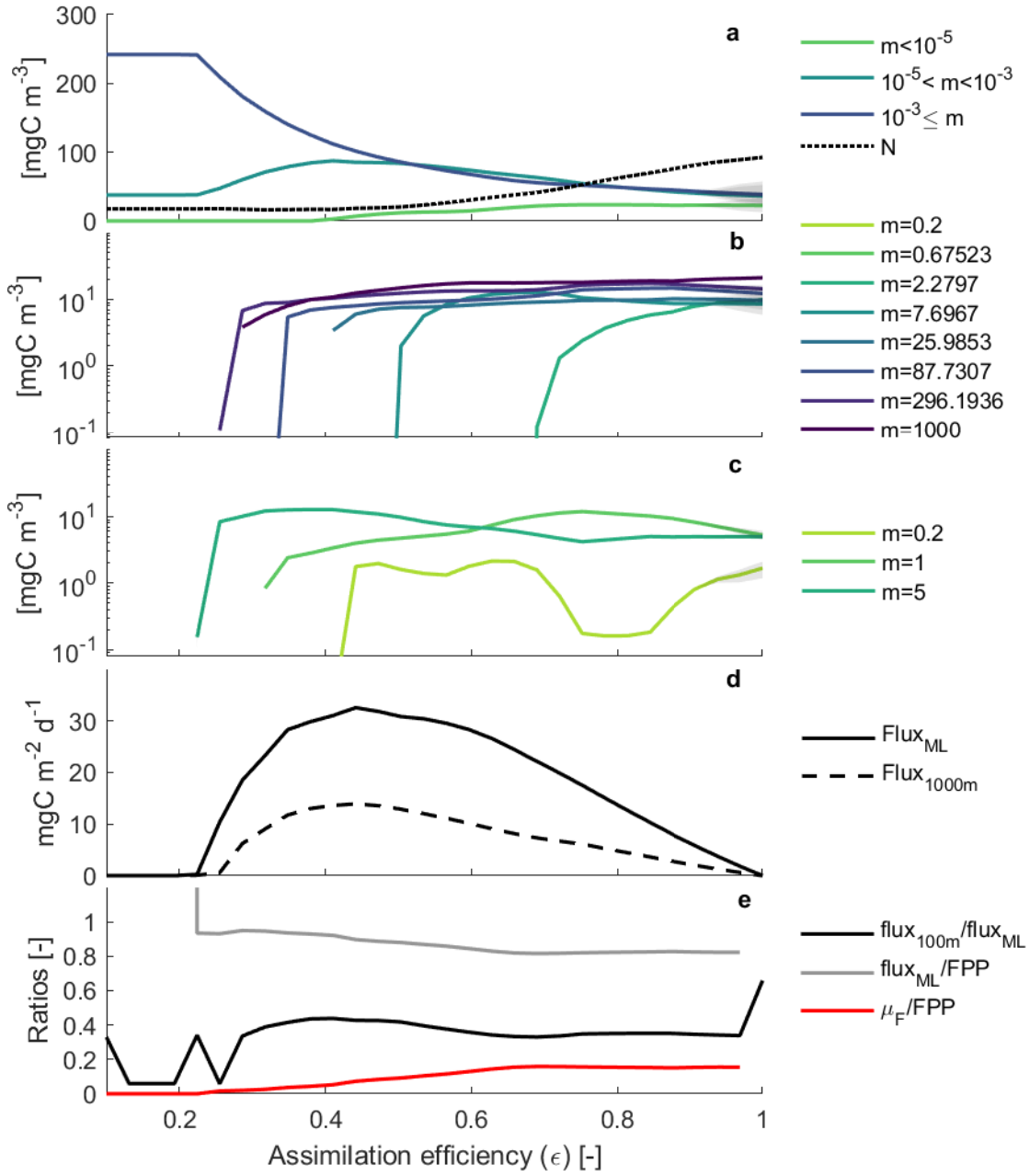

Fig. D.5. Parameter sweep for the assimilation efficiency (ϵ) of all copepods. (**a**) Protists grouped by size-ranges as stated in the legend. (**b**) active copepods and (**c**) passive copepods. Shaded areas around the lines show maximum and minimum biomass values when the system oscillates. (**d**) Fecal pellets export from the mixed layer ($Flux_{ML}$) and at 1000m ($Flux_{1000}$). (**e**) Transfer efficiency: fraction of pellets exported out of the mixed layer that reach 1000 m (black), fraction of fecal pellets produced that are exported out of the mixed layer (grey), and fraction of pellets produced that are consumed by copepods (red).

E Assumptions regarding large passive feeders

To our knowledge there are no passive feeding copepods that are large in size. Our assumption is that to be a passive feeder copepods need to be small to maintain neutral buoyancy. Even though for practical reasons we have decided to limit the size range of passive feeders to small copepods, the mechanism can be introduced, where both active and passive feeders can be run within the same size-ranges. In the following paragraphs we explain how could this mechanism be implemented in the model.

We introduce this mechanism via the parameter τ, which is the fraction of time that a copepod swims. Active feeders are constantly swimming to search for food, and therefore $\tau_{\text{act}} = 1$. For passive feeders, τ is size-dependent (Mauchline, 1998; Fig. E.1), where $\tau_{\text{pas}}(m)$ is 0 for small passive feeders and increases with the size of the copepod up to 1 for large passive feeders (Fig. E.1b).

Since large passive copepods need to swim continuously to counteract sinking, they have a respiration rate close to that of active feeders. The coefficient for the respiration rate from equations 2 ($\mu gC^{1/4}\ d^{-1}$) thus becomes dependent on τ and size:

$$\kappa(m) = \kappa_{\text{pas}} + \tau(m)(\kappa_{\text{act}} - \kappa_{\text{pas}}), \tag{E.1}$$

where κ_{pas} is the coefficient of the specific respiration rate of passive feeders, and κ_{act} of active feeders. Implementing the difference in respiration rates due to the feeding mode makes the critical feeding level of passive feeders mass-dependent and is higher for large copepods (Fig. 5).

Finally, passive feeding copepods have been suggested to experience predation mortality that is about 2 to 8 times lower than for active copepods (Almeda, van Someren Gréve, and Kiørboe, 2017). We implement this effect through the parameter c_{py}:

$$c_{\text{py}}(\tau_{\text{py}}, m_{\text{py}}) = \frac{1}{4} + \tau_{\text{py}}(m_{\text{py}})(1 - \frac{1}{4}), \tag{E.2}$$

This parameter is a sigmoid function which reduces predation mortality on small passive feeders by 1/3 (i.e. small passive feeders have a predation mortality 3 times lower), and approaches 1 as the size of copepods increases. This parameter is equivalent to 1 for active feeders.

E.0.1 Parameter τ

Sinking speed regression is $s_{\text{sink}} = 1.801L - 0.695$ where L is prosome length in mm Mauchline (1998). The regression of the swimming speed is $\log s_{\text{swim}} = 0.38 + 0.93 \log L$ from cruising velocity of pelagic copepods (Kiørboe et al., 2010).

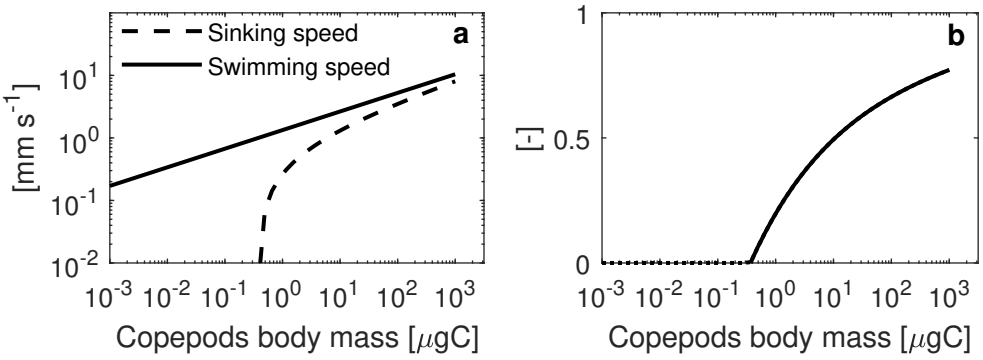

Fig. E.1. (**a**) Swimming and sinking speed of copepods (regressions obtained from Mauchline, 1998 (see appendix B for values) and (**b**) the ratio between sinking and swimming speeds (τ) are shown.

F Analytical solutions

F.1 Terminologies of size specta

In this article we will refer to three kinds of size spectra: the number spectrum, the biomass spectrum and the Sheldon spectrum. Different terminologies are used in different papers, so we here clarify our definitions and derivations:

- **Number spectrum**: number of individuals in a body-size range [or bin] divided by the body-size range. It may also be referred to as the *normalised* size spectrum (Sprules and Barth, 2016). Here the dimensions are in terms of abundance per body-mass: [individuals volume^{-1} body-mass^{-1}].

- **Biomass spectrum**: the biomass in a body-size range [or bin] divided by the body-size range. It is the same as the number spectrum but in terms of biomass. We can obtain it by multiplying the number spectrum with the corresponding body-mass. Here the dimensions are in terms of concentration per body-mass: [biomass volume^{-1} body-mass^{-1}].

- **Sheldon spectrum**: Represents the biomass in logarithmically-space body-size bin. It can be obtained from the biomass spectrum by multiplying with the bin width. Doing so makes the height of the spectrum depend on the bin width. To avoid this dependency we multiply with the body-mass. That gives the same scaling as multiplying by the bin width, since logarithmic bin widths are proportional to body mass. Here the dimensions are in [biomass volume^{-1}].

For a more detailed explanation see Andersen (2019) box 2.1 and figure 2.3.

F.2 Analytical solutions

We developed analytical solutions of the copepod model following Andersen and Beyer (2006) and Hartvig, Andersen, and Beyer (2011) while accounting for the determinate growth of copepods and their fixed adult:offspring size ratio. The derivations are made possible by some simplifying assumptions. The central assumption is that the feeding level is a constant, independent of the size of copepods: $f(m) = f_0$. The feeding level defines growth and by assuming that it is constant we can solve the growth equation for size-at-age, $m(t)$. Further, the feeding level of the predators determines their predation pressure on the prey. We can therefore also make simple solutions of the total size

spectrum of copepods and of the population growth rates of copepods. Before doing the full size spectrum calculations of the spectra we calculate solutions to the growth equation: size at age and development time from nauplii to adult copepod.

The size distribution of each population consists of a juvenile spectrum and an adult stage. Copepods have determinate growth, i.e., adults do not grow but invest net energy gain in reproduction. Therefore, the adult stage is a discrete size described as a delta-distribution:

$$N(m) = \underbrace{N_{\mathrm{juv}}(m)}_{\text{Spectrum juveniles}} + \underbrace{\delta(m - m_{\mathrm{a}})N_{\mathrm{a}}}_{\text{Adults}}, \tag{F.1}$$

where $\delta(m)$ is the Dirac delta function and N_{a} represents the adult spectrum. The Dirac delta-function ensures that the integral of the adult spectrum equals the adult abundance, even though the adult bin width is 0.

The spectrum of nauplii and copepodites $N_{\mathrm{juv}}(m)$ is a solution to the McKendric-von Foerster equation:

$$\underbrace{\frac{\partial N_{\mathrm{juv}}(m)}{\partial t}}_{\text{Dynamics over time}} + \underbrace{\frac{\partial g(m) m N_{\mathrm{juv}}(m)}{\partial m}}_{\text{Somatic growth}} = \underbrace{-\mu N_{\mathrm{juv}}(m)}_{\text{Losses}}, \tag{F.2}$$

where $g(m)$ is the net energy gain d^{-1} (5) that the juveniles use for somatic growth, and $\mu(m)$ is the total mortality. The number of adults is determined by the flux of juveniles becoming mature $N_{\mathrm{juv}}(m_{\mathrm{a}})g(m_{\mathrm{a}})$ and the losses to mortality $N_{\mathrm{a}}\mu(m_{\mathrm{a}})$:

$$\frac{\mathrm{d}N_{\mathrm{a}}}{\mathrm{d}t} = N_{\mathrm{juv}}(m_{\mathrm{a}})g(m_{\mathrm{a}}) - \mu(m_{\mathrm{a}})N_{\mathrm{a}}. \tag{F.3}$$

The boundary condition to equation (F.2) represents offspring production (Eq.7) by adults:

$$g m_0 N_{\mathrm{juv}}(m_0) = b N_{\mathrm{a}} \frac{m_{\mathrm{a}}}{m_0}. \tag{F.4}$$

The size spectrum represents the size distribution of individuals as a continuous number density distribution $N(m)$ with dimensions numbers per mass per volume (# µgC L^{-1}).

F.3 Growth

The growth rate of individuals (mass per time) is:

$$\dot{m}(t) = \nu(m)m = \underbrace{\epsilon h(f_0 - f_c)}_{A} m^{n+1} = Am^{n+1}, \tag{F.5}$$

following (4) with a constant feeding level f_0, and where we have defined the growth constant A. Solving for $m(t)$ gives:

$$m(t) = (m_0^{-n} - Ant)^{-1/n}. \tag{F.6}$$

As the growth constant, A, depends on the feeding level, so does the size at age $m(t)$ (Fig. 3B).

We find the development time from nauplii from (F.6) as the time where $m(t_{\text{adult}}) = m_{\text{a}}$:

$$t_{\text{adult}} = \frac{1 - z_{\text{a:o}}^{-n}}{An} m_0^{-n}, \tag{F.7}$$

where $z_{\text{a:o}} = m_a/m_0$ is the copepod-nauplii size ratio.

F.4 Size spectrum representation

The analytical calculations are performed on the copepod model formulated as a continuous size spectrum (F.20).

F.5 The total community size spectrum of copepods

First, we will calculate the community size spectrum, $N_{\text{c}}(m)$ of all copepods irrespective of their species, following Andersen and Beyer (2006) and Andersen (2019, Chap. 2). We make two assumptions: 1) that the community size spectrum is infinite and described as a power law: $N_{\text{c(m)}} = \kappa_{\text{c}} m^{-\lambda}$. This implies that we ignore the lower size limit of copepod eggs. 2) That the feeding level is constant, $f(m) = f_0$. Our aim is to determine the scaling exponent λ and the coefficient κ_c.

The encountered food $E_F(m)$ per mass is (14) (note that it is not the available food from eq.14):

$$E_F(m) = vm^q \int_0^\infty \phi(m_{\text{py}}, m) N_{\text{c}}(m_{\text{py}}) m_{\text{py}} \, \mathrm{d}m_{\text{py}}, \tag{F.8}$$

where vm^q is the specific clearance rate and ϕ is the size preference function (13). Inserting the ansatz for the community size spectrum and integrating gives:

$$E_F(m) = \alpha_{\mathrm{E}} v \kappa_{\mathrm{c}} m^{2+q-\lambda}, \quad \text{with } \alpha_{\mathrm{E}} = \sqrt{2\pi}\beta^{\lambda-2} \exp\left[(\lambda-2)^2\sigma^2/2\right], \tag{F.9}$$

where β is the preferred predator-prey mass ratio and σ the width of the preference function.

From the encountered food we can calculate the feeding level (1):

$$f(m) = \frac{E_F(m)}{E_F(m) + hm^n} = \frac{\alpha_{\mathrm{E}} v \kappa_{\mathrm{c}} m^{2+q-\lambda}}{\alpha_{\mathrm{E}} v \kappa_{\mathrm{c}} m^{2+q-\lambda} - hm^n}. \tag{F.10}$$

The only way for the feeding level to be constant (independent of mass) is if the two terms in the denominator are proportional to one another, i.e., if the encountered food is proportional to the specific maximum consumption rate hm^n. This condition implies that the two mass exponents are equal: $2 + q - \lambda = n$. From that condition we find that the exponent of the community size spectrum is $\lambda = 2 + q - n = 2$. As we have chosen q and n to be equal, the complicated exponential factors simplify, so that the encountered food is just $\alpha_{\mathrm{E}} = \sqrt{2\pi}\sigma$. If we know the constant feeding level $f(m) = f_0$, then we can further solve (F.10) for κ_{c}:

$$\kappa_{\mathrm{c}} = \frac{h}{v\alpha_{\mathrm{E}}} \frac{f_0}{1-f_0}. \tag{F.11}$$

Inserting κ_{c} and λ in the ansatz gives the community spectrum as:

$$N_{\mathrm{c}}(m) = \underbrace{\frac{1}{\alpha_{\mathrm{E}}} \frac{h}{v} \frac{f_0}{1-f_0}}_{\kappa_{\mathrm{c}}} m^{-2-q+n}. \tag{F.12}$$

F.6 Predation mortality

The predation mortality is imposed by all predators from the community feeding on prey of mass m_{py} with an effective clearance rate $(1-f_0)vm^q$ (Andersen and Beyer, 2006):

$$\mu_{\mathrm{p}}(m_{\mathrm{py}}) = \int_0^\infty (1-f_0) v m^{1+q} N_c(m) \phi(m_{\mathrm{py}}, m)\, \mathrm{d}m \tag{F.13}$$

$$= f_0 h \alpha_{\mathrm{E}}^{-1} m^n, \tag{F.14}$$

where the solution from (F.12) has been used. The predation mortality is declining with size with exponent n, and is proportional to the feeding level f_0 and the constant of maximum ingestion h; higher ingestion rates imply a larger mortality on the prey.

Size spectrum theory (Andersen and Beyer, 2006) operates with a dimensionless constant, the physiological mortality a, defined as the mortality divided by the specific growth rate:

$$a = \frac{\mu_{\mathrm{p}}}{Am^n} = \frac{f_0}{f_0 - f_c}\frac{1}{\epsilon\alpha_{\mathrm{E}}}. \tag{F.15}$$

The later analytical calculations are much simplified when they are formulated in terms of the physiological mortality.

F.7 The size spectrum of a copepod population

The spectrum of nauplii and copepodites $N(m)$ can be found as a solution to the McKendric-von Foerster equation (F.16) in steady state:

$$\frac{\mathrm{d}\nu(m)mN_{\mathrm{juv}}(m)}{\mathrm{d}m} = -\mu_{\mathrm{p}}N_{\mathrm{juv}}(m). \tag{F.16}$$

We know the growth rate from (F.5) and the mortality μ_{p} from (F.14) and (F.15): $\mu_{\mathrm{p}} = aAm^n$. Inserting in (F.2) gives:

$$N_{\mathrm{juv}}(m) = \kappa m^{-1-n-a}, \tag{F.17}$$

where κ is an integration constant.

The number of adults is given by a balance between the flux of maturing juveniles $N_{\mathrm{juv}}(m_{\mathrm{a}})\nu(m_{\mathrm{a}})m_a$ and the losses to mortality $N_{\mathrm{a}}\mu_{\mathrm{p}}(m_{\mathrm{a}})$:

$$N_{\mathrm{juv}}Am^{n+1} = N_{\mathrm{a}}\mu_{\mathrm{p}}(m_{\mathrm{a}}) \tag{F.18}$$

$$N_{\mathrm{a}} = \frac{\kappa}{a}m_{\mathrm{a}}^{-n-a}. \tag{F.19}$$

The combined juvenile and adult copepod spectrum is then:

$$N(m) = \kappa m^{-1-n-a}\left(1 + \frac{m_{\mathrm{a}}}{a}\delta(m_{\mathrm{a}})\right), \tag{F.20}$$

where $\delta(m_a)$ represents the Dirac delta function.

F.8 Copepod community structure

We can assemble the community spectrum N_c by summing up over all copepod spectra. This procedure will also give a specification of the integration constant $\kappa(m_a)$ as a function of the adult size.

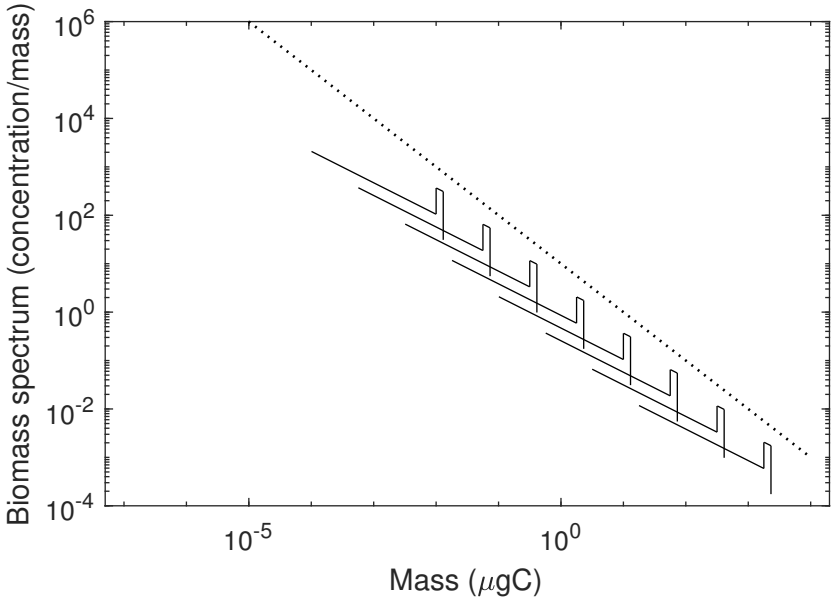

Fig. F.1. Spectra of the community (dotted) and copepods (continuous). The community spectrum is given by (F.12) with $\kappa_c = 1$. The copepod spectra each represent a range of adult sizes, which is why the adult range is not a delta-function (which cannot be plotted), but a range of sizes. Otherwise the spectra are as (F.24).

We can write the community spectrum as the integral over all copepod spectra with adult sizes in the range from m to mz:

$$N_{\mathrm{c}}(m) = \int_m^{mz} n(m)\,\mathrm{d}m_{\mathrm{a}}. \tag{F.21}$$

Inserting the community spectrum (F.12) and the solution of the population spectrum (F.20) gives:

$$\kappa_c m^{-2-q+n} = \int_m^{mz} \kappa(m_a) m^{-1-n-a} \left(1 + \frac{m_{\mathrm{a}}}{a}\delta(m_{\mathrm{a}})\right) \mathrm{d}m_a. \tag{F.22}$$

To evaluate the integral we need an assumption about the form of the integration constant $\kappa(m_a)$. We assume that it scales with adult mass with an exponent l: $\kappa(m_a) = \kappa_0 m_a^l$. Inserting in (F.22) and reducing gives:

$$\kappa_c m^{-2-q+n} = \kappa_0 m^{l-n-a} \underbrace{\left(z^{l+1} - 1\right)\left(\frac{1}{l+1} + \frac{1}{a}\right)}_{1/L}. \tag{F.23}$$

Equating the exponents of m on either side of the equation gives $l = 2n - 2 - q + a \approx a - 2.25$ and κ_0 as κ_{c} divided by the two parentheses on the right-hand-side. The first of the two parentheses represents the role of the adult-offspring mass ratio. The two terms in the second set of parentheses

are the contributions from the juvenile and adult populations. Defining $1/L$ as the product of the two parentheses on the right-hand-side we get the spectrum:

$$N(m,\, m_{\mathrm{a}}) = \kappa_{\mathrm{c}} L m_{\mathrm{a}}^{2n-2-q+a} m^{-1-n-a}. \tag{F.24}$$

Notice that the spectrum is now the combination of a size distribution – the dependency on m – and a trait distribution – the dependency on m_{a} (Fig. F.1). The dimensions are therefore numbers per body mass per adult body mass.

F.9 Maximum population growth rate

When a population does not experience density dependent effects it will grow at the maximum population growth rate $r_{\max}$. This derivations follows Andersen, 2019 chapter 7.1. We can find $r_{\max}$ by solving the time-dependent McKendric-von Foerster equation (F.2). Note that we expect growth $g(m) = \nu(m)m$ and mortality $\mu_p(m)$ to be constant in time. Our solution will follow the procedure in (Andersen, 2019, Chap. 7). First we write an ansatz for the solution as:

$$N(m,t) = Ke^{r_{\max}t}\mathcal{N}(m). \tag{F.25}$$

This ansatz separates the variables of time and mass. Note that the mass-dependent part, $\mathcal{N}(m)$, is not the same as the previous solution (F.20), which was a steady-state solution.

Inserting the ansatz (F.25) and $\nu(m)m = Am^{n+1}$ and $\mu_p(m) = aAm^n$ in (F.2) and solving for $\mathcal{N}(m)$ gives:

$$\mathcal{N}(m) = \kappa m^{-1-n-a} \exp\left[\frac{r_{\max}}{nA} m^{-n}\right], \tag{F.26}$$

where κ is again an unknown integration constant. As before we have the adult copepods as $N_a(t) = N(m_a,t)m_a/a$. We can now determine the population growth rate $r_{\max}$ by applying the boundary condition that the flux of nauplii $\epsilon_R \nu(m_a) m_a N_a(t)/m_0$ equals the flux at the smallest size $\nu(m_0)m_0 N(m_0,t)$ to find:

$$r_{\max} = Am_a^n \frac{n}{z_{\mathrm{a:o}}^n - 1}\left[(1-a)\ln(z_{\mathrm{a:o}}) + \ln(\epsilon_R/a)\right], \tag{F.27}$$

where $z_{\mathrm{a:o}} = m_a/m_0$ is again the mass ratio between copepods and nauplii. We see that the population growth rate increases with the growth rate coefficient A and metabolically with adult size. The

term in the brackets is a correction factor which decreases as the reproductive efficiency ϵ_{r} decreases and as the physiological mortality a increases, i.e., if mortality increases or growth decreases.

F.10 Equilibrium values of physiological mortality and feeding level

The value of $r_{\max}$ is the population growth rate in the absence of density dependent effects. Density dependence will change the growth and mortality rates of the copepods until the population is in equilibrium. Changes in growth and mortality are represented through the physiological mortality a, which is the ratio between mortality and growth (F.15). Density-dependent effects will reduce the actual population growth rate from $r_{\max}$ until it is exactly zero, where the population is in equilibrium. From (33) we see that this happens when the term in the brackets is zero. That point defines the equilibrium level of the physiological mortality $\overline{a}$:

$$(1-\overline{a})\ln(z_{\mathrm{a:o}}) + \ln(\epsilon_{\mathrm{r}}/\overline{a}) = 0. \tag{F.28}$$

This is a transcendental equation, which cannot be solved in closed form. The value for active and passive copepods is $\overline{a} = 0.85$ and 0.76. Inserting the relation between a and the feeding level f_0 from (F.15) we can solve for the equilibrium feeding level; we find $\overline{f}_0 = 0.4$ and 0.83 respectively. The equilibrium feeding level for active copepods fits quite well with the observed emergent feeding level from the numerical calculations (Fig. 5C+D). The equilibrium feeding level for passive feeders is much higher, which indicates that passive should not be able to persist at all. However, this calculation has not factored in the reduced predation pressure on passive feeders (E.2). If we assume that the predation pressure is shaped by the active feeders, but that this predation is reduced by a factor three on passive ($\tau = 0$ in Eq. E.2) we find $\overline{f}_0 = 0.13$. This is a much smaller feeding level, which explains why small passive feeders are able to persist, in particular under low food conditions.

G Error function

We used the error function in the prey preference function to correct for the size bins. The error function integrates the preference function within the range of the size bin, which is needed if the bins are wide. The error function is:

$$\mathrm{erf}(x) = \frac{2}{\sqrt{\pi}} \int_0^{\infty} \exp(-t^2) \mathrm{d}t \tag{G.1}$$

Therefore, the preference function of a given predator with stage width ranging from m_i to m_{i+1} becomes:

$$\Phi = \frac{\sqrt{\frac{\pi}{2}}\sigma_c \left[\mathrm{erf}\left(\frac{(\log(m_i) - \log(\frac{m_{\mathrm{pred}}}{\beta}))}{\sqrt{2}\sigma} \right) - \mathrm{erf}\left(\frac{(\log(m_{i+1}) - \log(\frac{m_{\mathrm{pred}}}{\beta}))}{\sqrt{2}\sigma} \right) \right]}{\log(m_i) - \log(m_{i+1})}; \tag{G.2}$$

H Supplementary figures

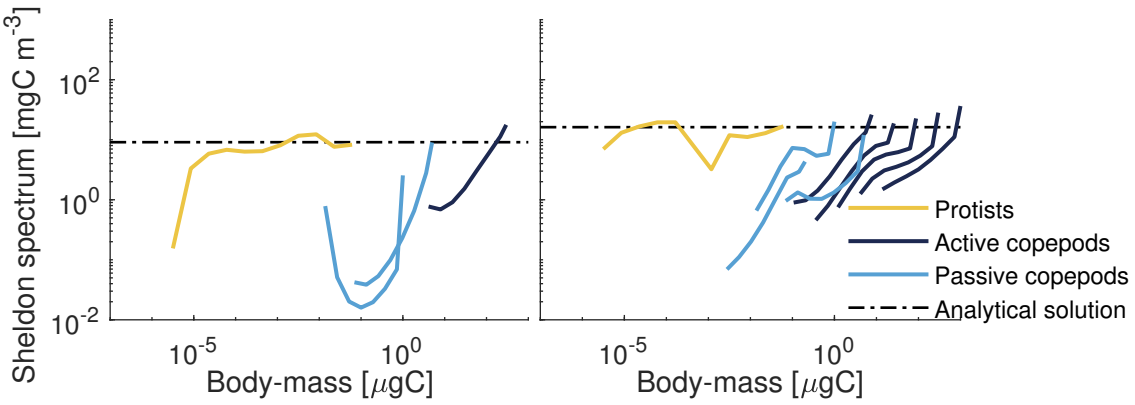

Fig. H.1. Sheldon spectrum from figure 5, left panel has low inputs of nitrogen ($\rho = 0.005$ d^{-1}) and right side panel is for high inputs of nitrogen ($\rho = 0.05$ d^{-1}). The Sheldon was simply derived by multiplying the biomass spectrum by m (or the number spectrum by m^2, as explained in Andersen, 2019 chapter 2 Box 1).

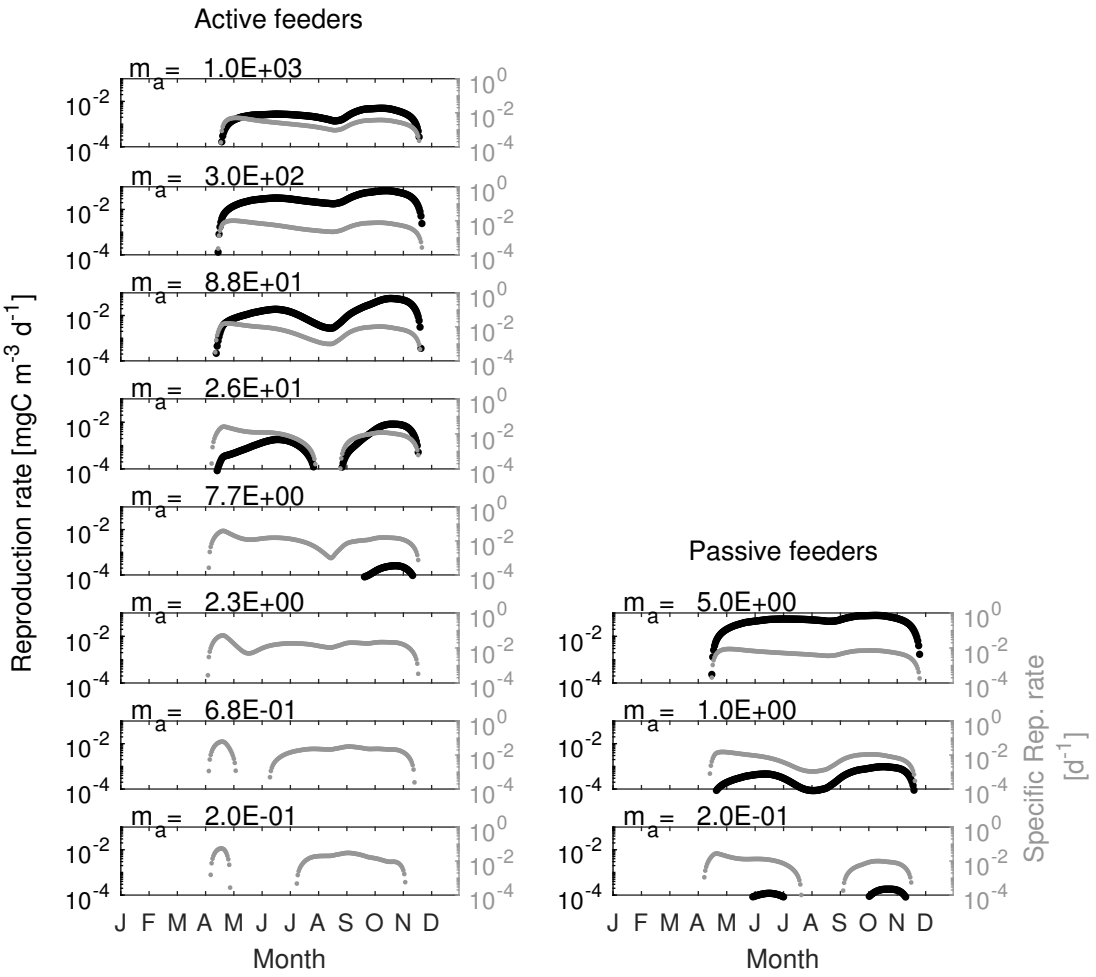

Fig. H.2. Total reproduction (left y-axis in black) and specific reproduction rates (right y-axis in grey) of all copepods in the seasonal environment. Left side panels is for active copepods, right side panels is for passive copepods. The lower panels are small copepods and the upper panels large copepods following the adult sizes (m_a in µgC) written on top of each panel.

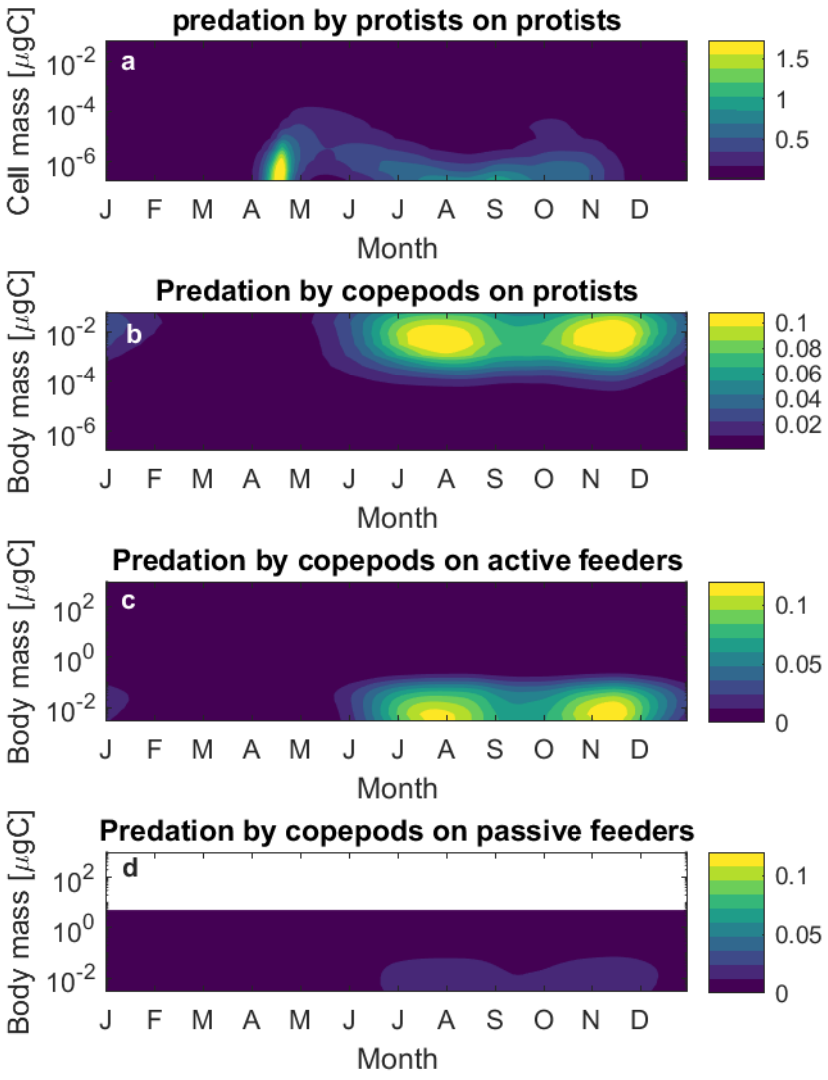

Fig. H.3. Predations (d^{-1}) in the seasonal scenario fro protists and copepods. Y-axys is the body-mass of the prey. (a) predation by protists on protists. (b) predation by all copepods on protists. (c) predation by copepods on active copepods. (d) predation by copepods on passive copepods. Colormap of panels c and d are in Log_{10}, explaining the negative values in the colorbar.

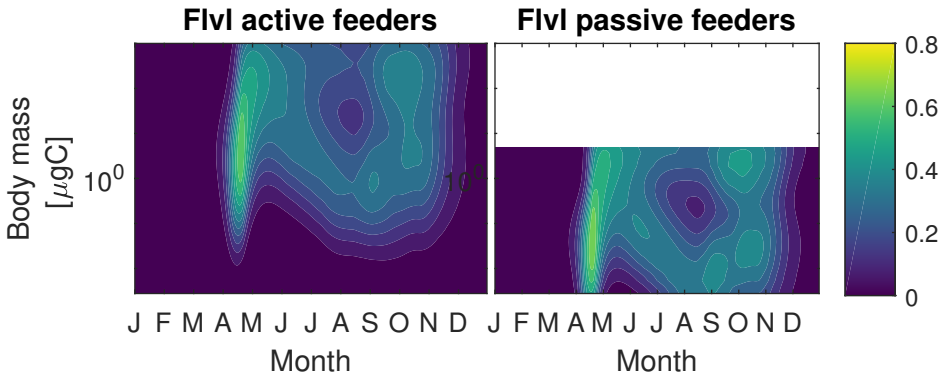

Fig. H.4. Feeding level in the seasonal scenario for active and passive copepods.

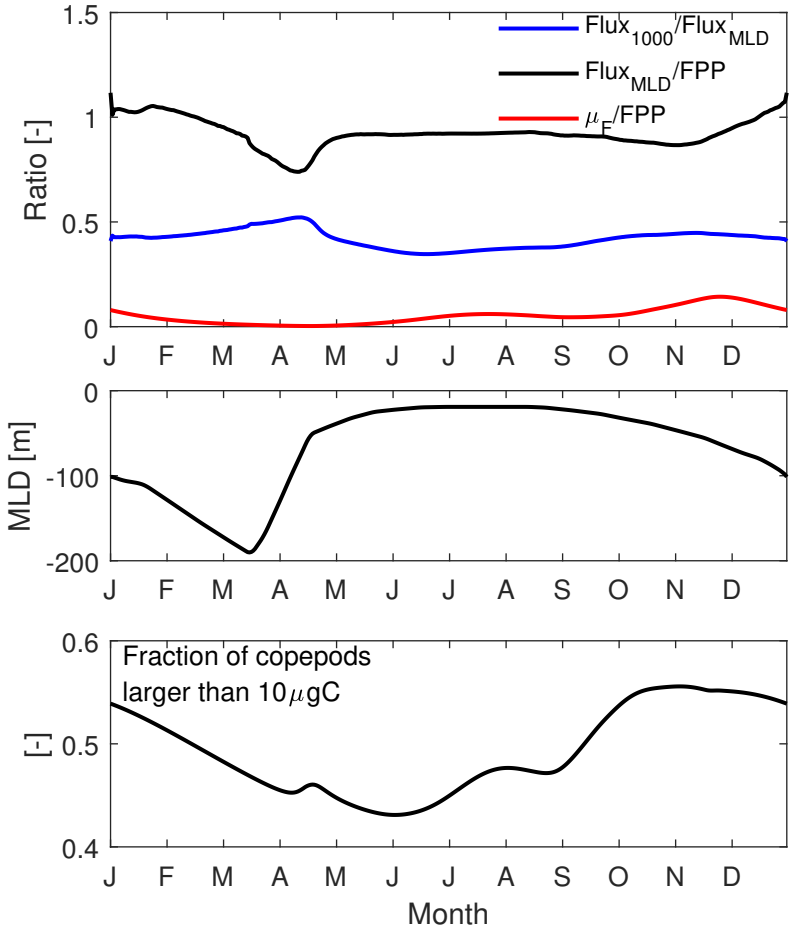

Fig. H.5. Diagnostic related to fecal pellets export in the seasonal scenario. Upper panel: Fraction of fecal pellets out of the mixed layer exported to a 1000 m (black), fraction of fecal pellets exported out of the mixed layer relative to fecal pellets production rate (FPP) within the mixed layer (grey), and fraction of fecal pellets consumed (μ_F) relative to the fecal pellets production rate (red). Middles panel: mixed layer depth. Lower panel= fraction of copepods larger than 10 µgC relative to the whole community.

References

Almeda, Rodrigo, Hans van Someren Gréve, and Thomas Kiørboe (2017). "Behavior is a major determinant of predation risk in zooplankton". In: *Ecosphere* 8.2, e01668.

Andersen, Ken H (2019). *Fish Ecology, Evolution, and Exploitation: A New Theoretical Synthesis*. Vol. 93. Monographs in Population Biology. Princeton University Press.

Andersen, Ken Haste and Jan E Beyer (2006). "Asymptotic size determines species abundance in the marine size spectrum". In: *The American Naturalist* 168.1, pp. 54–61.

Andersen, Ken Haste et al. (2008). "Life-history constraints on the success of the many small eggs reproductive strategy". In: *Theoretical population biology* 73.4, pp. 490–497.

Andersen, Ken Haste et al. (2016). "Characteristic sizes of life in the oceans, from bacteria to whales". In:

Chisholm, Laurie A and John C Roff (1990). "Size-weight relationships and biomass of tropical neritic copepods off Kingston, Jamaica". In: *Marine Biology* 106.1, pp. 71–77.

Edwards, Kyle F, Christopher A Klausmeier, and Elena Litchman (2015). "Nutrient utilization traits of phytoplankton". In: *Ecology* 96.8, pp. 2311–2311.

Elliott, JM and W Davison (1975). "Energy equivalents of oxygen consumption in animal energetics". In: *Oecologia* 19.3, pp. 195–201.

Evans, Geoffrey T and John S Parslow (1985). "A model of annual plankton cycles". In: *Biological oceanography* 3.3, pp. 327–347.

Fasham, MJR, HW Ducklow, and SM McKelvie (1990). "A nitrogen-based model of plankton dynamics in the oceanic mixed layer". In: *Journal of Marine Research* 48.3, pp. 591–639.

Hansen, Benni, Peter Koefoed Bjornsen, and Per Juel Hansen (1994). "The size ratio between planktonic predators and their prey". In: *Limnology and oceanography* 39.2, pp. 395–403.

Hartvig, Martin, Ken H Andersen, and Jan E Beyer (2011). "Food web framework for size-structured populations". In: *Journal of theoretical Biology* 272.1, pp. 113–122.

Ikeda, Tsutomu, Atsushi Yamaguchi, and Takashi Matsuishi (2006). "Chemical composition and energy content of deep-sea calanoid copepods in the Western North Pacific Ocean". In: *Deep Sea Research Part I: Oceanographic Research Papers* 53.11, pp. 1791–1809.

Kiørboe, T and Marina Sabatini (1995). "Scaling of fecundity, growth and development in marine planktonic copepods". In: *Marine ecology progress series. Oldendorf* 120.1, pp. 285–298.

Kiørboe, Thomas (2016). "Foraging mode and prey size spectra of suspension-feeding copepods and other zooplankton". In: *Marine Ecology Progress Series* 558, pp. 15–20.

Kiørboe, Thomas and Andrew G Hirst (2014). "Shifts in mass scaling of respiration, feeding, and growth rates across life-form transitions in marine pelagic organisms". In: *The American Naturalist* 183.4, E118–E130.

Kiørboe, Thomas, Flemming Møhlenberg, and Kirsten Hamburger (1985). "Bioenergetics of the planktonic copepod Acartia tonsa: relation between feeding, egg production and respiration, and composition of specific dynamic action". In: *Mar Ecol Prog Ser* 26.1-2, pp. 85–97.

Kiørboe, Thomas and Marina Sabatini (1994). "Reproductive and life cycle strategies in egg-carrying cyclopoid and free-spawning calanoid copepods". In: *Journal of Plankton Research* 16.10, pp. 1353–1366.

Kiørboe, Thomas et al. (2010). "Unsteady motion: escape jumps in planktonic copepods, their kinematics and energetics". In: *Journal of the Royal Society Interface* 7.52, pp. 1591–1602.

Marañón, Emilio et al. (2013). "Unimodal size scaling of phytoplankton growth and the size dependence of nutrient uptake and use". In: *Ecology letters* 16.3, pp. 371–379.

Mauchline, John (1998). "The biology of calanoid copepods". In: *Adv. Mar. Biol.* 33, pp. 1–710.

Menden-Deuer, Susanne and Evelyn J Lessard (2000). "Carbon to volume relationships for dinoflagellates, diatoms, and other protist plankton". In: *Limnology and oceanography* 45.3, pp. 569–579.

Neuheimer, A. B. et al. (2015). "Adult and offspring size in the ocean over 17 orders of magnitude follows two life-history strategies". In: *Ecology* 96.12, pp. 3303–3311.

Small, LF, SW Fowler, and MY Ünlü (1979). "Sinking rates of natural copepod fecal pellets". In: *Marine Biology* 51.3, pp. 233–241.

Sprules, William Gary and Lauren Emily Barth (2016). "Surfing the biomass size spectrum: some remarks on history, theory, and application". In: *Canadian Journal of Fisheries and Aquatic Sciences* 73.4, pp. 477–495.

Ward, Ben A et al. (2017). "The size dependence of phytoplankton growth rates: a trade-off between nutrient uptake and metabolism". In: *The American Naturalist* 189.2, pp. 170–177.